



# Conformational flexibility in amidophosphoesters: a CSD analysis completed with two new crystal structures of $(\text{C}_6\text{H}_5\text{O})_2\text{P}(\text{O})\text{X}$ [ $\text{X} = \text{NHC}_7\text{H}_{13}$ and $\text{N}(\text{CH}_2\text{C}_6\text{H}_5)_2$ ]

Banafsheh Vahdani Alviri,<sup>a</sup> Mehrdad Pourayoubi,<sup>a\*</sup> Abdul Ajees Abdul Salam,<sup>b\*</sup> Marek Nečas,<sup>c</sup> Arie van der Lee,<sup>d</sup> Akshara Chithran<sup>b</sup> and Krishnan Damodaran<sup>e</sup>

Received 7 August 2019

Accepted 10 December 2019

Edited by Y. Ohgo, Teikyo University, Japan

**Keywords:** amidophosphoester; conformational flexibility; Cambridge Structural Database; crystal structure; hydrogen bonding; energy framework.

**CCDC references:** 1971119; 1895358

**Supporting information:** this article has supporting information at journals.iucr.org/c

<sup>a</sup>Department of Chemistry, Faculty of Science, Ferdowsi University of Mashhad, Mashhad, Iran, <sup>b</sup>Department of Atomic and Molecular Physics, Centre for Applied Nanosciences, Manipal Academy of Higher Education, Manipal, Karnataka 576 104, India, <sup>c</sup>Department of Chemistry, Masaryk University, Kotlarska 2, 61137 Brno, Czech Republic, <sup>d</sup>Institut Européen des Membranes, Université de Montpellier, 34095 Montpellier, France, and <sup>e</sup>Department of Chemistry, University of Pittsburgh, Pittsburgh, PA 15260, USA. \*Correspondence e-mail: pourayoubi@um.ac.ir, abdul.ajeas@manipal.edu

The crystal structures of diphenyl (cycloheptylamido)phosphate,  $\text{C}_{19}\text{H}_{24}\text{NO}_3\text{P}$  or  $(\text{C}_6\text{H}_5\text{O})_2\text{P}(\text{O})(\text{NHC}_7\text{H}_{13})$ , (**I**), and diphenyl (dibenzylamido)phosphate,  $\text{C}_{26}\text{H}_{24}\text{NO}_3\text{P}$  or  $(\text{C}_6\text{H}_5\text{O})_2\text{P}(\text{O})[\text{N}(\text{CH}_2\text{C}_6\text{H}_5)_2]$ , (**II**), are reported. The  $\text{NHC}_7\text{H}_{13}$  group in (**I**) provides two significant hydrogen-donor sites in  $\text{N}-\text{H}\cdots\text{O}$  and  $\text{C}-\text{H}\cdots\text{O}$  hydrogen bonds, needed for a one-dimensional hydrogen-bond pattern along [100] in the crystal, while (**II**), with a  $(\text{C}_6\text{H}_5\text{CH}_2)_2\text{N}$  moiety, lacks these hydrogen bonds, but its three-dimensional supramolecular structure is mediated by  $\text{C}-\text{H}\cdots\pi$  interactions. The conformational behaviour of the phenyl rings in (**I**), (**II**) and analogous structures from the Cambridge Structural Database (CSD) were studied in terms of flexibility, volume of the other group attached to phosphorus and packing forces. From this study, synclinal ( $\pm sc$ ), anticlinal ( $\pm ac$ ) and antiperiplanar ( $\pm ap$ ) conformations were found to occur. In the structure of (**II**), there is an intramolecular  $\text{C}_{ortho}-\text{H}\cdots\text{O}$  interaction that imposes a  $+sc$  conformation for the phenyl ring involved. For the structures from the CSD, the  $+sc$  and  $\pm ap$  conformations appear to be mainly imposed by similar  $\text{C}_{ortho}-\text{H}\cdots\text{O}$  intramolecular interactions. The large contribution of the  $\text{C}\cdots\text{H}/\text{H}\cdots\text{C}$  contacts (32.3%) in the two-dimensional fingerprint plots of (**II**) is a result of the  $\text{C}-\text{H}\cdots\pi$  interactions. The differential scanning calorimetry (DSC) analyses exhibit peak temperatures ( $T_m$ ) at 109 and 81 °C for (**I**) and (**II**), respectively, which agree with the strengths of the intermolecular contacts and the melting points.

## 1. Introduction

Conformational studies are of great interest not only due to their importance in biological systems and drug design but also for purely scientific considerations, such as the study of nonrigid segments in the solid state and in solution (Mattern *et al.*, 2000; Hopfinger & Battershell, 1976; Fang *et al.*, 2014; Gholivand & Pourayoubi, 2004). The relationship between conformational behaviour and molecular packing has been extensively studied, and there are many examples of conformations imposed by intra- and intermolecular interactions and conformational preferences, typically in organotin systems (Buntine *et al.*, 1998), amides and acids (Dauber & Hagler, 1980) and polypeptide chains (Gregoret & Cohen, 1991). The effect of conformational flexibility on the existence of two (or more) symmetry-independent molecules in the crystal, disordered structures and the formation of polymorphs were also

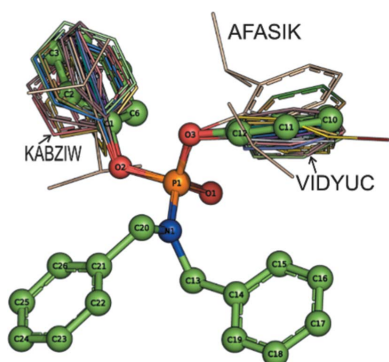
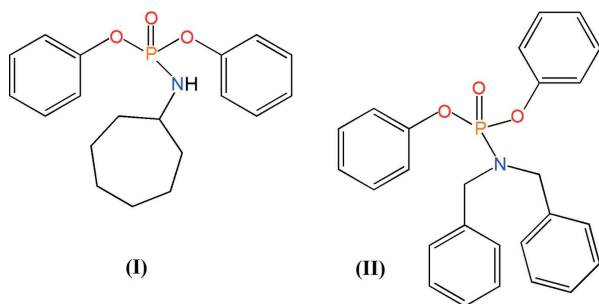


**Table 1**  
Experimental details.

	(I)	(II)
Crystal data		
Chemical formula	C <sub>19</sub> H <sub>24</sub> NO <sub>3</sub> P	C <sub>26</sub> H <sub>24</sub> NO <sub>3</sub> P
<i>M<sub>r</sub></i>	345.36	429.43
Crystal system, space group	Orthorhombic, <i>Pna</i> 2 <sub>1</sub>	Triclinic, <i>P</i> $\bar{1}$
Temperature (K)	175	120
<i>a</i> , <i>b</i> , <i>c</i> (Å)	9.3538 (2), 9.7899 (3), 19.3432 (5)	8.3404 (3), 9.5349 (5), 14.9677 (7)
$\alpha$ , $\beta$ , $\gamma$ (°)	90, 90, 90	76.280 (4), 75.778 (4), 72.055 (4)
<i>V</i> (Å <sup>3</sup> )	1771.31 (5)	1080.73 (9)
<i>Z</i>	4	2
Radiation type	Mo <i>K</i> $\alpha$	Mo <i>K</i> $\alpha$
$\mu$ (mm <sup>-1</sup> )	0.17	0.16
Crystal size (mm)	0.35 × 0.25 × 0.15	0.25 × 0.20 × 0.20
Data collection		
Diffractometer	Rigaku Xcalibur Sapphire3 Gemini	AFC11 (Right): Eulerian 3 circle CCD
Absorption correction	Multi-scan ( <i>CrysAlis PRO</i> ; Rigaku OD, 2015)	Multi-scan ( <i>CrysAlis PRO</i> ; Rigaku OD, 2015)
<i>T</i> <sub>min</sub> , <i>T</i> <sub>max</sub>	0.979, 1.000	0.722, 1.000
No. of measured, independent and observed reflections [ <i>I</i> > 2 $\sigma$ ( <i>I</i> )]	9026, 3411, 2964	9523, 3901, 3578
<i>R</i> <sub>int</sub>	0.035	0.018
( <i>sin</i> $\theta$ / $\lambda$ ) <sub>max</sub> (Å <sup>-1</sup> )	0.660	0.602
Refinement		
<i>R</i> [ <i>F</i> <sup>2</sup> > 2 $\sigma$ ( <i>F</i> <sup>2</sup> )], <i>wR</i> ( <i>F</i> <sup>2</sup> ), <i>S</i>	0.052, 0.103, 0.95	0.033, 0.086, 1.05
No. of reflections	3338	3901
No. of parameters	221	280
No. of restraints	79	0
H-atom treatment	H atoms treated by a mixture of independent and constrained refinement	H-atom parameters constrained
$\Delta\rho_{\max}$ , $\Delta\rho_{\min}$ (e Å <sup>-3</sup> )	0.32, -0.54	0.27, -0.34
Absolute structure	Flack (1983), 1505 Friedel pairs	–
Absolute structure parameter	0.6 (3)	–

Computer programs: *CrysAlis PRO* (Rigaku OD, 2015), *CrystalClear-SM Expert* (Rigaku, 2011), *SUPERFLIP* (Palatinus & Chapuis, 2007), *SHELXT2014* (Sheldrick, 2015a), *CRYSTALS* (Betteridge *et al.*, 2003), *SHELXL2018* (Sheldrick, 2015b), *CAMERON* (Watkin *et al.*, 1996) and *pyMOL* (Schrödinger, 2015).

studied (Toghraee *et al.*, 2011; Keikha *et al.*, 2017; Vahdani Alviri *et al.*, 2018; Bernstein & Hagler, 1978).



The Cambridge Structural Database (CSD; Version 5.40, updated to November 2018; Groom *et al.*, 2016) provides the opportunity to study conformational behaviour in analogous structures; in some recently published articles, we investigated conformational changes, typically in P(O)NHC(O)-based structures (Toghraee *et al.*, 2011; Vahdani Alviri *et al.*, 2018) and phosphate salts (Moghaddam *et al.*, 2019), where, for example, the orientation of P(O) versus C(O) groups, the ring conformations of four-, five-, six- and seven-membered aliphatic rings, and the conformational flexibility of aliphatic and aromatic rings with respect to the other segments in the molecule/salt were considered.

With this background in mind, we present here the synthesis, crystal structure and spectroscopic characterization of

two amidophosphoesters with the same (C<sub>6</sub>H<sub>5</sub>O)<sub>2</sub>P(O) fragment and different in the type of amine fragment attached to phosphorus, in order to study conformational changes driven by the substituent effect and packing forces made by classical and/or nonclassical hydrogen bonds. The compounds are (C<sub>6</sub>H<sub>5</sub>O)<sub>2</sub>P(O)(NHC<sub>7</sub>H<sub>13</sub>), (**I**), and (C<sub>6</sub>H<sub>5</sub>O)<sub>2</sub>P(O)[N(CH<sub>2</sub>-C<sub>6</sub>H<sub>5</sub>)<sub>2</sub>], (**II**) (see Scheme). The conformational flexibilities of the rings in (**I**) and (**II**), and analogous structures deposited in the CSD were investigated. The Hirshfeld surfaces, electrostatic energy frameworks and DSC analyses also detailed in this article.

## 2. Experimental

Previous articles have described the synthesis of compounds (**I**) and (**II**) from the reaction between diphenylphosphoryl chloride and cycloheptylamine in the presence of neutral alumina (Al<sub>2</sub>O<sub>3</sub>) for (**I**) and from the reaction of [DBNP(O)(OPh)<sub>2</sub>]PF<sub>6</sub> (DBN = *N*-acyl-1,5-diazabicyclo[4.3.0]non-5-ene) and dibenzylamine in CH<sub>3</sub>CN medium for (**II**). Melting points, selected IR bands and mass peaks for both (**I**) and (**II**), and <sup>31</sup>P and <sup>1</sup>H NMR data for (**I**) in CDCl<sub>3</sub>, and <sup>31</sup>P, <sup>1</sup>H and <sup>13</sup>C NMR data for (**II**) in acetone-*d*<sub>6</sub> were reported (Gupta *et al.*, 2005, 2007; Jones *et al.*, 2016). Here we report the single-crystal X-ray diffraction analysis and some complementary spectroscopic features for (**I**) and (**II**). The NMR

experiments were studied again in a different solvent (*i.e.* DMSO- $d_6$ ).

## 2.1. Synthesis

**2.1.1. Synthesis of  $(C_6H_5O)_2P(O)(NHC_7H_{13})$ , (I).** Compound **(I)** was prepared from the reaction of diphenylphosphoryl chloride and cycloheptylamine (1:2 molar ratio, reaction time 4 h, ice-bath temperature) in dry  $CHCl_3$ . The solvent was removed in a vacuum and the solid which formed was washed with distilled water. Colourless single crystals suitable for X-ray analysis were obtained at room temperature from a mixture of  $CH_3OH$  and  $CHCl_3$  (4:1 *v/v*).

Analytical data: colourless prism-shaped crystal; m.p. 109 °C. IR (KBr,  $cm^{-1}$ ): 3240, 3052, 2918, 2860, 1591, 1488, 1317, 1242, 1196, 1162, 1075, 1013, 929, 894, 826, 779, 744, 686, 651.  $^{31}P\{^1H\}$  NMR (243 MHz, DMSO- $d_6$ ):  $\delta$  -0.41.  $^1H$  NMR (601 MHz, DMSO- $d_6$ ):  $\delta$  1.25–1.33 (*m*, 2H), 1.35–1.45 (*m*, 4H), 1.45–1.56 (*m*, 4H), 1.67–1.75 (*m*, 2H), 3.19–3.29 (*m*, 1H), 5.80 (*dd*,  $J = 13.7, 9.7$  Hz, 1H, NH), 7.19 (*t*,  $J = 7.4$  Hz, 2H), 7.21–7.25 (*m*, 4H), 7.36–7.42 (*m*, 4H).  $^{13}C\{^1H\}$  NMR (151 MHz, DMSO- $d_6$ ):  $\delta$  23.20, 27.61, 36.71 (*d*,  $J = 5.3$  Hz), 52.84, 120.12 (*d*,  $J = 4.9$  Hz), 124.62, 129.71, 150.79 (*d*,  $J = 6.4$  Hz). MS (70 eV, EI):  $m/z$  (%) = 345 (2) [ $M$ ] $^+$ , 344 (18) [ $M - 1$ ] $^+$ , 286 (100) [ $M - C_4H_{10} - H$ ] $^+$ , 248 (56) [ $M - C_7H_{13}$ ] $^+$ .

**2.1.2. Synthesis of  $(C_6H_5O)_2P(O)[N(CH_2C_6H_5)_2]$ , (II).** Compound **(II)** was prepared from the reaction of diphenylphosphoryl chloride and dibenzylamine (1:2 molar ratio, reaction time 4 h, ice-bath temperature) in dry  $CHCl_3$ . The solvent was removed in a vacuum and the solid which formed was washed with distilled water. Colourless single crystals suitable for X-ray analysis were obtained at room temperature from a mixture of  $CHCl_3$  and  $CH_3CN$  (4:1 *v/v*).

Analytical data: colourless block-shaped crystal; m.p. 81 °C. IR (KBr,  $cm^{-1}$ ): 3434, 2999, 2790, 2630, 2483, 1745, 1629, 1592, 1490, 1454, 1369, 1244, 1210, 1099, 1017, 915, 751, 692.  $^{31}P\{^1H\}$  NMR (122 MHz, DMSO- $d_6$ ):  $\delta$  -11.63.  $^1H$  NMR (301 MHz, DMSO- $d_6$ ):  $\delta$  4.10 (*m*, 4H,  $CH_2$ ), 6.98–7.03 (*m*, 2H), 7.15–7.18 (*m*, 4H), 7.22–7.29 (*m*, 4H), 7.39–7.40 (*m*, 2H), 7.40–7.43 (*m*, 4H), 7.50–7.54 (*m*, 4H).  $^{13}C\{^1H\}$  NMR (76 MHz, DMSO- $d_6$ ):  $\delta$  50.35, 120.38 (*d*,  $J = 5.3$  Hz), 122.66, 129.07, 129.34, 129.43, 130.52, 132.36, 154.05 (*d*,  $J = 6.8$  Hz). MS (70 eV, EI):  $m/z$  (%) = 430 (54) [ $M + 1$ ] $^+$ , 429 (52) [ $M$ ] $^+$ , 428 (23) [ $M - 1$ ] $^+$ , 336 (100) [ $M - OPh$ ] $^+$ , 243 (36) [ $M - 2 OPh$ ] $^+$ , 91 (95) [ $C_7H_7$ ] $^+$ .

## 2.2. Refinement

Crystal data, data collection, and structure refinement details are summarized in Table 1. The *ab initio* iterative charge-flipping method was used to solve the crystal structure of **(I)**; the parameters are described elsewhere (van der Lee, 2013). For both **(I)** and **(II)**, all carbon-bound H atoms were placed at calculated positions and refined as riding, with  $U_{iso}(H)$  values set at  $1.2U_{eq}$  of the respective carrier atoms. However, the position of atom H171 was refined with a soft distance and two angle restraints with respect to the parent N17 atom. All soft restraints used in these refinements have

been described by Waser (1963) and Rollet (1965). The standard uncertainty (s.u.) used for the N–H distance restraint was 0.02 Å and for the two angle restraints was 2°. The structure of **(I)** was refined in the space group  $Pn2_1a$  as an inversion twin; the structure solution in the centrosymmetric space group  $Pnma$  was investigated but was found to be much more disordered with respect to the cycloheptane ring than the model in  $Pn2_1a$ . The latter model is, however, not completely free from disorder, as is shown in the displacement ellipsoid plot (Fig. 1). A model with the cycloheptane ring disordered over two distinct positions was not significantly better than the model shown in Fig. 1, so the undisordered model was preferred, using some soft distance restraints (with an s.u. of 0.01 Å), as well as restraints on the atomic displacement parameters for the atoms in the cycloheptane ring. The s.u. values for the vibration restraints were taken between 0.001 and 0.005 Å<sup>2</sup>, and for the thermal similarity restraints between 0.01 and 0.02 Å<sup>2</sup>. The Flack (1983) parameter refined to 0.6 (3) and an *a posteriori* Hooft analysis based on maximum likelihood estimation and Bayesian statistics gave a probability of the chance of having a racemic twin of 99.86%, with a Hooft parameter of 0.6 (1) (Hooft *et al.*, 2008).

## 3. Results and discussion

### 3.1. Structural description

The asymmetric units of amidophosphoesters  $(C_6H_5O)_2P(O)(NHC_7H_{13})$ , **(I)**, and  $(C_6H_5O)_2P(O)[N(CH_2C_6H_5)_2]$ , **(II)**, consist of one complete molecule (Figs. 1 and 2). Selected geometric parameters and hydrogen-bond geometries of **(I)** and **(II)** are presented in Tables 2–5. In both structures, the P atoms are within a distorted tetrahedral  $(O)_2(N)P(O)$  environment, with the angles at the P atoms ranging from 93.42 (10) to 115.5 (3)° for **(I)** and from 97.78 (5) to 116.27 (5)° for **(II)**. The extreme values correspond to the O2–P1–O10 and O9–P1–O10 angles for **(I)**, and the O2–P1–O3 and O1–

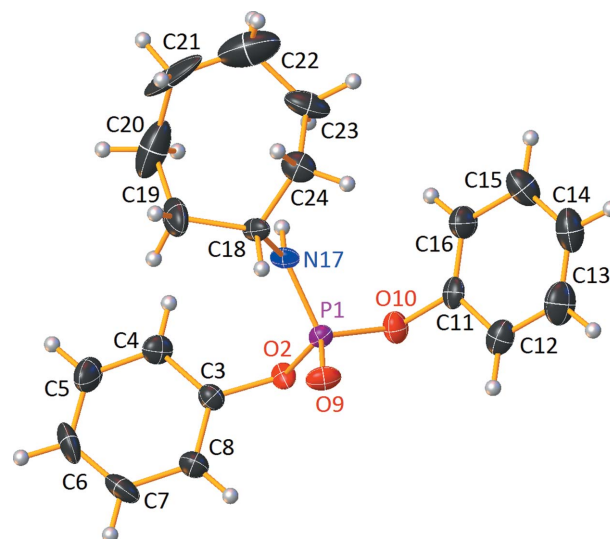


**Figure 1**  
Displacement ellipsoid plot (50% probability level) for **(I)**, showing the atom-numbering scheme.

**Table 2**  
Selected geometric parameters (Å, °) for **(I)**.

P1—O2	1.601 (3)	O2—C3	1.405 (6)
P1—O9	1.4645 (18)	O10—C11	1.399 (6)
P1—O10	1.581 (4)	N17—C18	1.479 (3)
P1—N17	1.607 (2)		
O2—P1—O9	114.8 (3)	O10—P1—N17	109.2 (2)
O2—P1—O10	93.42 (10)	P1—O2—C3	120.7 (3)
O9—P1—O10	115.5 (3)	P1—O10—C11	119.7 (3)
O2—P1—N17	108.8 (2)	P1—N17—C18	124.57 (17)
O9—P1—N17	113.34 (11)		

**Table 3**  
Hydrogen-bond geometry (Å, °) for **(I)**.

<i>D</i> —H... <i>A</i>	<i>D</i> —H	H... <i>A</i>	<i>D</i> ... <i>A</i>	<i>D</i> —H... <i>A</i>
C23—H232...O9 <sup>i</sup>	0.97	2.57	3.516 (8)	166 (1)
N17—H171...O9 <sup>i</sup>	0.86	2.08	2.901 (8)	159 (4)

Symmetry code: (i)  $x + \frac{1}{2}, -y + \frac{3}{2}, z$ .

P1—O3 angles for **(II)**. The sum of the surrounding angles at the N atom, *i.e.* C—N—P + P—N—H + H—N—C for **(I)**, shows a difference of about 2.5° with respect to the bond-angle sum for ideal  $sp^2$  hybridization (360°), while the bond-angle sum of  $2 \times \text{P—N—C} + \text{C—N—C}$  for **(II)** shows a practically planar environment at the N atom.

The P=O bond lengths [1.4645 (18) Å for **(I)** and 1.4578 (10) Å for **(II)**] are comparable to those in analogous compounds (Sabbaghi *et al.*, 2019) and are slightly longer than the normal P=O double-bond length (1.45 Å; Corbridge, 1995). The P—N bond lengths [1.607 (2) Å for **(I)** and 1.6232 (11) Å for **(II)**] are standard for structures with an (O)<sub>2</sub>P(O)(N) skeleton (Sabbaghi *et al.*, 2019) and are smaller than a typical P—N single-bond length (Corbridge, 1995).

The P—O—C bond angles are 120.7 (3) (P1—O2—C3) and 119.7 (3)° (P1—O10—C11) in **(I)**, and 122.79 (8) (C1—O2—

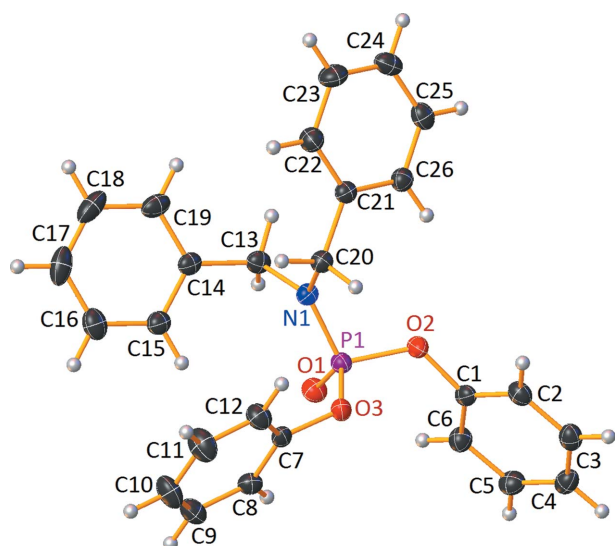


**Figure 2**  
Displacement ellipsoid plot (50% probability level) for **(II)**, showing the atom-numbering scheme.

**Table 4**  
Selected geometric parameters (Å, °) for **(II)**.

P1—O1	1.4578 (10)	O2—C1	1.4092 (15)
P1—O2	1.5916 (9)	O3—C7	1.4096 (15)
P1—O3	1.5948 (10)	N1—C13	1.4693 (17)
P1—N1	1.6232 (11)	N1—C20	1.4707 (17)
O1—P1—O2	115.77 (5)	C1—O2—P1	122.79 (8)
O1—P1—O3	116.27 (5)	C7—O3—P1	119.73 (8)
O2—P1—O3	97.78 (5)	C13—N1—C20	115.99 (10)
O1—P1—N1	113.54 (6)	C13—N1—P1	121.10 (9)
O2—P1—N1	104.31 (5)	C20—N1—P1	122.88 (9)
O3—P1—N1	107.44 (5)		

**Table 5**  
Hydrogen-bond geometry (Å, °) for **(II)**.

Cg1, Cg2 and Cg3 are the centroids of the C1—C6, C14—C19 and C7—C12 rings, respectively.

<i>D</i> —H... <i>A</i>	<i>D</i> —H	H... <i>A</i>	<i>D</i> ... <i>A</i>	<i>D</i> —H... <i>A</i>
C2—H2A...Cg1 <sup>i</sup>	0.95	3.50	3.9798 (13)	114
C13—H13B...Cg1 <sup>ii</sup>	0.99	3.49	4.2048 (13)	131
C18—H18A...Cg3 <sup>iii</sup>	0.95	3.22	3.8839 (15)	128
C8—H8A...Cg2 <sup>iii</sup>	0.95	3.41	3.7716 (14)	106
C6—H6A...O1	0.95	2.51	3.1488 (17)	125

Symmetry codes: (i)  $-x, -y + 1, -z + 1$ ; (ii)  $x, y - 1, z$ ; (iii)  $-x + 1, -y, -z$ .

P1) and 119.73 (8)° (C7—O3—P1) in **(II)** indicate an  $sp^2$ -hybridization state for the O atoms, similar to the P—O—C angles in analogous structures with similar P(Y)(O—C)<sub>2</sub>(N) (Y = O and S) skeletons (Sabbaghi *et al.*, 2016).

The similar torsion angles describing the environment around the P—N unit are close to each other for the two compounds. Thus, the O9—P1—N17—C18 torsion angle [0.96 (7)°] in **(I)** is close to the O1—P1—N1—C13 torsion angle [−4.83 (12)°] in **(II)** and, similarly, O2—P1—N17—C18 [129.9 (5)°] and O10—P1—N17—C18 [−129.4 (5)°] of **(I)** are close to the O2—P1—N1—C13 [122.07 (10)°] and O3—P1—N1—C13 [−134.84 (10)°] torsion angles of **(II)**, respectively. In addition to these, the O9—P1—N17—H171 (162.39°), O2—P1—N17—H171 (−68.65°) and O10—P1—N17—H171 (32.05°) torsion angles of **(I)** have values close to the O1—P1—N1—C20 [173.29 (10)°], O2—P1—N1—C20 [−59.82 (11)°] and O3—P1—N1—C20 [43.28 (11)°] torsion angles of **(II)**, respectively. On the other hand, the C20 atom of **(II)** occupies the equivalent position to the H171 atom of **(I)**.

In the next section, the conformations of the phenyl rings in **(I)** and **(II)** and the varieties of conformations observed in analogous structures available in the CSD are investigated in order to depict a comparative study and understand the effects of substitution and packing forces on the conformations of the phenyl rings.

### 3.2. CSD analysis

**3.2.1. Comparative studies with analogous compounds available in the CSD.** The bond lengths of the 162 molecules obtained from the CSD were extracted (see Table S1 in the supporting information) and the averages of the bond lengths were compared with similar bond lengths in title compounds

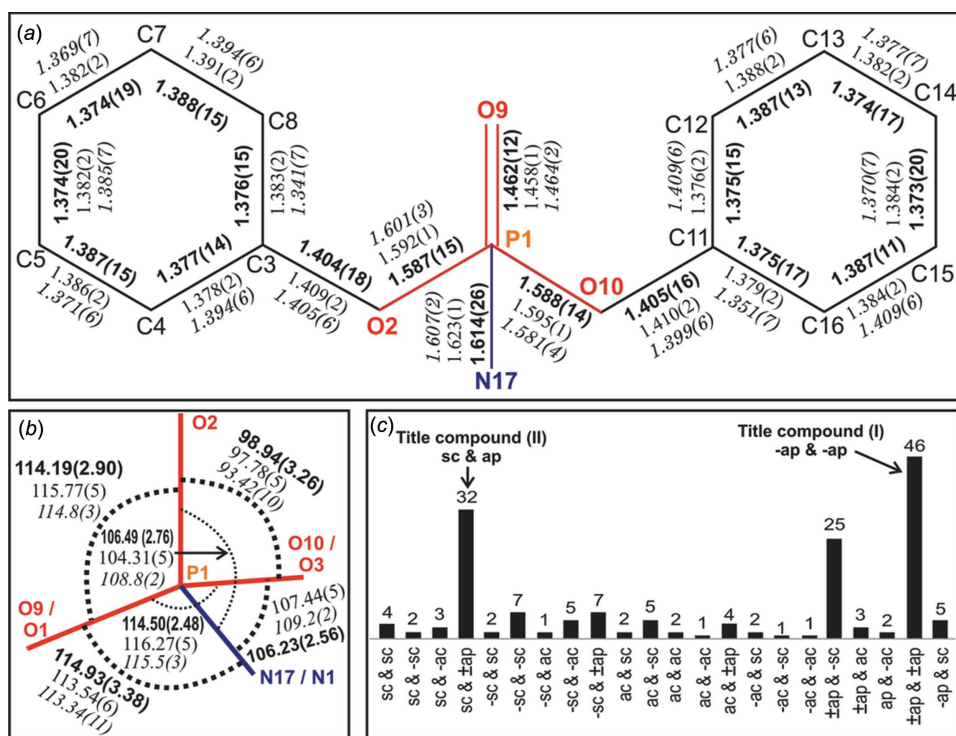


Figure 3

Comparative study of the title compounds with similar structures available in the CSD. (a) The averages of the bond lengths calculated from the 162 molecules containing the P(O)(OPh)<sub>2</sub>N skeleton are shown with the bond lengths of the title compounds. The atom numbering for (I) is shown for reference. The bond lengths of the CSD structures and compounds (I) and (II) are shown in bold, italic and normal fonts, respectively. (b) The average bond angles at the P atom calculated for the 162 molecules are shown with the bond angles of the title compounds. The bold fonts represent the average bond angles calculated from structures extracted from the CSD. The italic and normal fonts represent the data for (I) and (II), respectively. (c) The conformational summary of the two phenyl rings attached to the ester O atoms. The phenyl rings of (I) adopt *-ap* and *-ap* conformations, and those of (II) adopt *+sc* and *+ap* conformations, and their respective positions are marked and shown with an arrow.

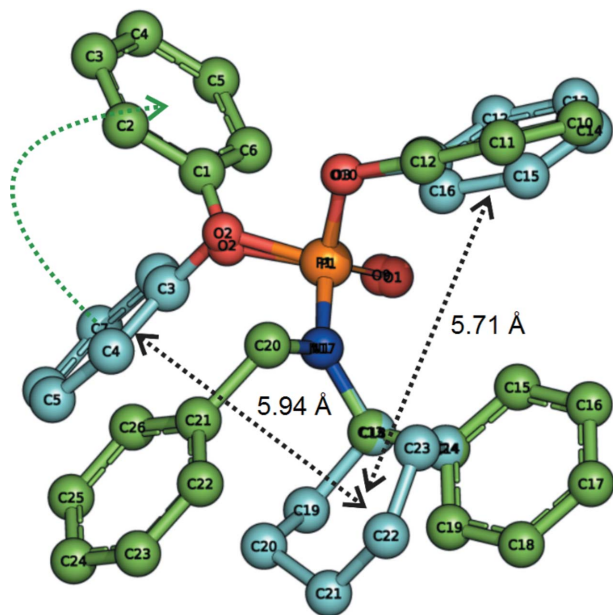


Figure 4

Superposition of compounds (I) and (II), both shown in a ball-and-stick model and with C atoms coloured cyan for (I) and green for (II). The O, N and P atoms are coloured red, blue and orange, respectively. The distance between the two phenyl rings from the seven-membered ring of (I) is marked. The conformational change of phenyl ring 1 of (II) in comparison with a similar ring in (I) is shown with a green arrow.

(I) and (II) (Fig. 3a). The bond lengths of (I) and (II) match with each other, as well as with the calculated averages (Fig. 3a). Slight but not significant variations are observed for (I) with respect to the C3–C4, C3–C8, C11–C12 and C11–C16 bonds, and all other bond lengths match with the standard deviations of the average values. In terms of bond angles, six were measured at the P atom and the data are listed in Table S2 in the supporting information. The averages of the bond angles calculated from the CSD structures are highly correlated with the title compounds, except for O2–P1–O10 of (I), which is smaller than all the other bond angles (Fig. 3b), due to the effect of the neighbouring bulky cycloheptyl ring. A comparative analysis of torsion angles/conformations was also provided which will be discussed in the next section (Fig. 3c and Table S3 in the supporting information).

Compounds (I) and (II) were superimposed with eight atoms constituting the (CCO)(O)P(O)(NC) skeleton [*i.e.* O2, P1, O9, O10, N17, C11, C16, and C18 of (I), and O2, P1, O1, O3, N1, C7, C12 and C13 of (II)], with an r.m.s. deviation of 0.08 Å. Phenyl rings C11–C16 of (I) and C7–C12 of (II) adopt a similar antiperiplanar (*ap*) conformation with a slight difference in the orientation [*-ap* for (I) and *+ap* for (II)]. The conformation is considered based on the C–O–P–O torsion angle and the angles ranging from  $\pm 150$  to  $180^\circ$  denote an  $\pm ap$  conformation. The seven-membered ring (atoms C18–C24) of (I) is closely aligned with the C14–C19 phenyl ring of (II)

(Fig. 4). From the viewpoint of conformational changes, the significant difference between the two compounds arises due to the bulky C21–C26 phenyl-ring substituent at the N atom in (II). To accommodate this phenyl ring, another phenyl ring (C1–C6) rotates away and adopts a synclinal position (+*sc*), compared with an *−ap* orientation for the corresponding phenyl ring in (I). The distances between the rings are gathered in Table S4 of the supporting information. In (I), the seven-membered ring is located between the phenyl rings at almost equal distances from both, *viz.* 5.94 Å from phenyl ring C3–C8 and 5.71 Å from phenyl ring C11–C16 (see Fig. 4 and Table S4 in the supporting information).

**3.2.2. The phenyl-ring conformations.** In the previous section, the *−ap* conformation for phenyl rings 1 (atoms C3–C8) and 2 (C11–C16) of (I), and the +*sc* and +*ap* conformations, respectively, for phenyl rings 1 (C1–C6) and 2 (C7–C12) of (II) were introduced. Based on the torsion angles, the 162 molecules extracted from the CSD are divided into 22 groups. The *−ap* and +*ap* conformations are consistent with a *trans* orientation, so they can be combined together for a comparative study (Fig. 3*c*). From Fig. 3(*c*) and Table S3 in the supporting information, it is evident that 32 structures adopt +*sc* and ±*ap* conformations, and 46 structures adopt ±*ap* and ±*ap* conformations. Fig. 5(*a*) shows the superposition of the

CSD structures corresponding to (I) and (II) with the structures of the title structures.

In (I), the angle between the planes of the phenyl rings is 26.1 (3)° and the torsion angles of  $-178.2$  (4)° for C3–O2–P1–O10 and  $-179.7$  (4)° for C11–O10–P1–O2 define the *−ap* conformation for phenyl rings 1 and 2, as noted. The 14 molecules ZIFYIW-Mol1 (Aparna *et al.*, 1995), LEQRIK01-Mol2 (Gholivand *et al.*, 2013), YEVSAT (Herrmann *et al.*, 1994), FIBROY-Mol1 (Gholivand *et al.*, 2005), OFESEZ-Mol2 (Safin *et al.*, 2013), BIFYUN (Das *et al.*, 2018), BIFXIA-Mol1 (Das *et al.*, 2018), BOGPOC (Drewelies & Pritzkow, 1982), UREDUR-Mol1 (Sabbaghi *et al.*, 2011*b*), KAVVAE-Mol1 (Zák *et al.*, 1989), SOYCUE-Mol1 (Richter *et al.*, 1991), SOYCUE-Mol2 (Richter *et al.*, 1991), OFESAV-Mol1 (Safin *et al.*, 2013) and WIBKUN-Mol1 (Rebrova *et al.*, 1993) adopt a similar conformation (*−ap* and *−ap*) and their phenyl rings are similar to those in (I) (Fig. 5*b* and Table S3 in the supporting information). There are slight variations in some structures due to torsion-angle variations and bulk substitution in the phenyl rings or at the N atom, which are common and have been observed in previously reported structures (Simon *et al.*, 2017). For example, YEVSAT and FIBROY-Mol1 have methyl substitution at the 4-position in the phenyl rings. Due to this effect, the phenyl rings are slightly disor-

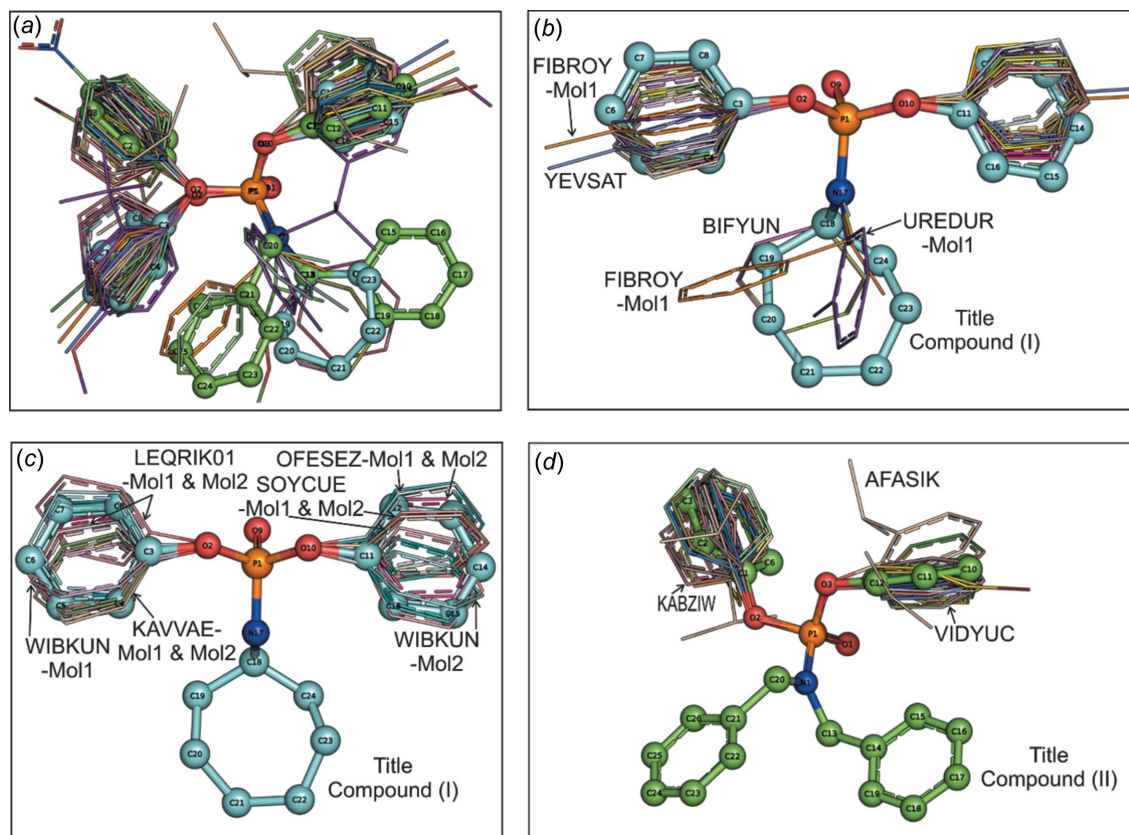


Figure 5

The conformational flexibility of the title compounds and the CSD structures. (*a*) The CSD structures corresponding to compounds (I) and (II) are shown along with (I) and (II), which are coloured as in Fig. 4. (*b*) Superposition of the CSD structures, which belong to the *−ap* and *−ap* conformations, along with compound (I), with slightly deviating structures marked. (*c*) Representative structures that adopt ±*ap* conformations in comparison with compound (I). (*d*) Superposition of the CSD structures which belong to the +*sc* and ±*ap* conformations, along with compound (II). For clarity, the P(O)(OPh)<sub>2</sub>N skeletons of the CSD structures have been retained and other substitutions have been removed for most of the structures.

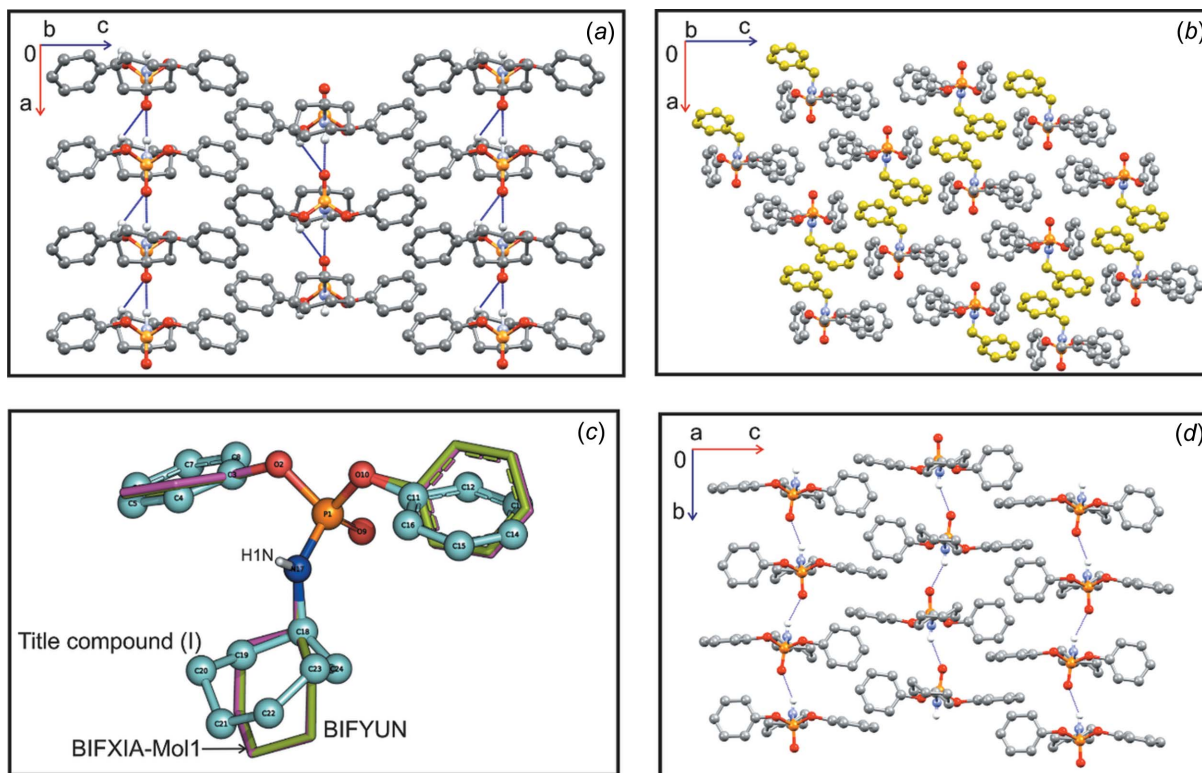


Figure 6

The packing diagrams of (a) **(I)** and (b) **(II)**, viewed along the *b* axis. For clarity, H atoms not involved in molecular interactions have been omitted in part (a) and all H atoms have been omitted in part (b). The additional phenyl ring available in **(II)**, which is in the equivalent position of the H atom of N–H in **(I)**, is shown in green. (c) Superposition of **(I)** with the CSD structures (refcodes BIFXIA\_Mol1 and BIFYUN). Both BIFXIA\_Mol1 and BIFYUN adopt similar conformations to compound **(I)**. The two structures contain a six-membered ring instead of the seven-membered ring present in **(I)**. (d) The molecular packing diagram of BIFYUN, viewed along the *a* axis. The N–H···O hydrogen-bond pattern of **(I)** shown in part (a) is similar to that in BIFYUN.

oriented with respect to the other structures. Similarly, UREDUR-Mol1 and FIBROY-Mol1 have a bulky phenyl group attached at an N-atom position and, due to this substitution, the phenyl rings are slightly twisted in comparison with the other structures.

As was discussed earlier, the  $\pm ap$  conformations adopt a similar *trans* orientation. For example, OFESAV-Mol1 adopts  $-ap$  and  $-ap$  conformations, and OFESAV-Mol2 adopts  $+ap$  and  $+ap$  conformations, and both molecules are perfectly aligned with each other, as well as with compound **(I)**. Similarly, KAVVAE-Mol1 ( $-ap/-ap$ ), KAVVAE-Mol2 ( $+ap/+ap$ ), LEQRIK01-Mol1 ( $+ap/+ap$ ), LEQRIK01-Mol2 ( $-ap/-ap$ ),

SOYCUE-Mol1 ( $-ap/-ap$ ), SOYCUE-Mol2 ( $-ap/-ap$ ), WIBKUN-Mol1 ( $-ap/-ap$ ) and WIBKUN-Mol2 ( $+ap/+ap$ ), which adopt  $\pm ap$  conformations, also fit well with **(I)** (Fig. 5c).

In **(II)**, the planes of the phenyl rings make a dihedral angle of  $59.40(5)^\circ$ , which is  $\sim 33^\circ$  greater than the corresponding angle in **(I)**. There are 11 molecules in the CSD with conformations like those observed in **(II)** (*i.e.*  $+sc$  and  $+ap$ ). These are WEWVUP (Allcock *et al.*, 1994), WIHPIM (Balakrishna *et al.*, 1994), UCOHID (Necas *et al.*, 2001), UCOFOH-Mol1 (Necas *et al.*, 2001), NOKHOL (Endeshaw *et al.*, 2008), XABSEZ (Rybarczyk-Pirek *et al.*, 2002a), OVUXAF-Mol2 (Chandrasekaran *et al.*, 2011), MOPMIN (Rybarczyk-Pirek *et al.*, 2002b), UCOHAV-Mol3 (Necas *et al.*, 2001), NACJOR (Cadierno *et al.*, 2004a) and BACVEH-Mol1 (Du *et al.*, 2001), and there is no remarkable difference between these 11 molecules and **(II)**.

Due to the similar orientation of the  $\pm ap$  conformation, the  $+sc$  and  $-ap$  conformations are also aligned well with compound **(II)**. There are 21 structures which adopt  $+sc$  and  $-ap$  conformations (Table S3 in the supporting information). For example, AFASIK (Krishna *et al.*, 2007), VIDYUC (Ammon *et al.*, 1991) and KABZIW (Attanasi *et al.*, 1988) can also be superimposed with compound **(II)**, and all are perfectly aligned with **(II)** (Fig. 5d). From the CSD comparison results, a *trans* ( $\pm ap$ ) conformation is one of the preferred conforma-

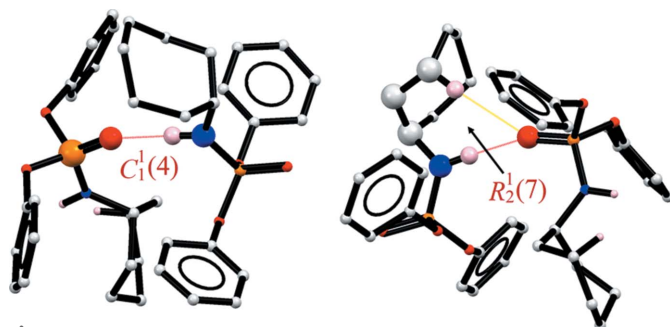


Figure 7  
The graph-set motifs in **(I)**.

tions for the two phenyl rings in molecules with the  $P(O)(OPh)_2N$  skeleton. Out of 162 molecules, 46 molecules adopt  $\pm ap/\pm ap$  conformations, which are similar to compound **(I)** (Fig. 3c). Similarly, 32 molecules adopt  $sc$  and  $\pm ap$  conformations, which are similar to compound **(II)**. The next most frequent conformations (25 molecules) are  $\pm ap$  and  $-sc$ , which are the preferred alternative conformations similar to compound **(II)**. Thus, for 124 out of 162 molecules either both phenyl rings or one of the phenyl rings adopts a *trans* conformation (Fig. 3c and Table S3 in the supporting information).

**3.2.3. Intra- and intermolecular interactions.** In the crystal of **(I)**, adjacent molecules are linked through moderate  $N-H\cdots O$  and weak  $C-H\cdots O$  intermolecular hydrogen bonds, forming a linear arrangement along the *a* axis (Fig. 6a). The  $NHC_7H_{13}$  group provides the two donor sites needed for these two hydrogen bonds. Compound **(II)** lacks an  $N-H$  group and a seven-membered ring, which prevents the formation of similar hydrogen bonds, except for the  $C6-H6A\cdots O1$  intramolecular hydrogen bond with an angle of  $125^\circ$ . This structure possesses more phenyl rings than that of **(I)**, and its three-dimensional (3D) supramolecular assembly is built from  $C-H\cdots\pi$  interactions (Table 5). Fig. 6(b) shows a view of the crystal packing in the structure of **(II)**.

It is quite interesting that the recently published structure of diphenylcyclohexyl aminophosphonate (CSD refcodes BIFXIA and BIFYUN) is the closest structure to **(I)**. The reference structure (Das *et al.*, 2018) has a six-membered ring attached to the N atom, while compound **(I)** has a seven-membered ring. Both structures can be superimposed well, and the H atom attached to the N atom is oriented on the same side (Fig. 6c). The  $N-H\cdots O$  hydrogen-bond pattern and the molecular packing of BIFYUN resemble those in compound **(I)** (Fig. 6d).

Another feature of the intramolecular interactions is related to the phenyl-ring conformation (with the assistance of the bulk effect, which was discussed previously). In the structure of **(II)**, the phenyl ring with the  $+sc$  conformation is the one involved in intramolecular  $C-H\cdots O$  hydrogen bonding. A CSD survey reveals that it is quite common that the O atom of the  $P=O$  group is involved in intramolecular  $C-H\cdots O$  interactions with one of the phenyl rings when it adopts an  $+sc$  or  $\pm ap$  conformation. For example, the typical structures with the CSD refcodes XABSEZ, UCOHAV-Mol3, QABZIF (Warren *et al.*, 2016), IYAMEA-Mol1 (Cadierno *et al.*, 2004b) and EROJAX (Sabbaghi *et al.*, 2011a) form intramolecular  $C-H\cdots O=P$  hydrogen bonds with an angle of  $\sim 125^\circ$ .

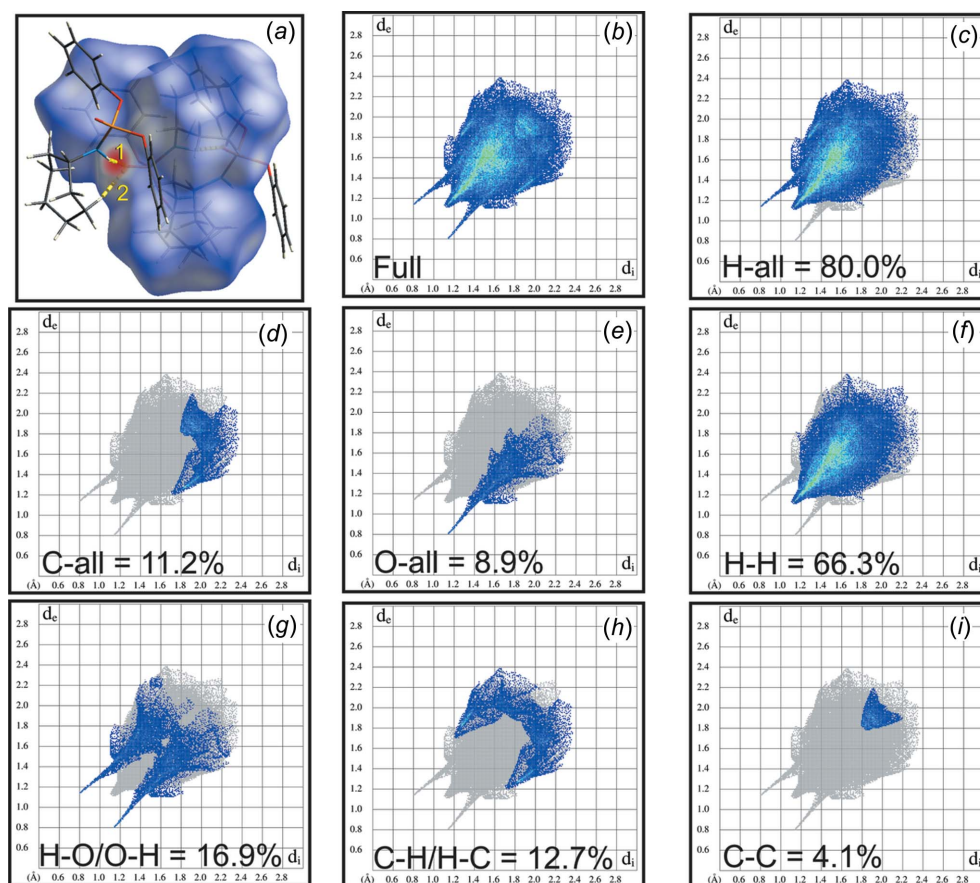


**Figure 8**

(a) Hirshfeld surface (HS) for structure **(I)** (mapped with  $d_{\text{norm}}$ ). Labels on the HS are as follows:  $N17-H171\cdots O9=P1$  (**1**) and  $C23-H232\cdots O9=P1$  (**2**). 2D fingerprint plots of **(I)** for (b) full, (c)  $H\cdots All$ , (d)  $C\cdots All$ , (e)  $O\cdots All$ , (f)  $H\cdots H$ , (g)  $O\cdots H/H\cdots O$ , (h)  $C\cdots H/H\cdots C$  and (i)  $C\cdots C$ . The contributions of P and N (0%) are not shown.

The hydrogen-bond network of **(I)** includes  $R_2^1(7)$  and  $C(4)$  graph-set motifs, as shown in Fig. 7 (for graph-set notation, see Bernstein *et al.*, 1995).

### 3.3. Hirshfeld surface analysis

**3.3.1. Hirshfeld surface maps and fingerprint plots.** The intermolecular interactions of **(I)** and **(II)** were further studied by Hirshfeld surface (HS) analysis, including 3D HS maps, two-dimensional (2D) fingerprint (FP) plots and electrostatic energy frameworks. The HSs mapped with  $d_{\text{norm}}$  and the corresponding shape-index-associated 2D FP plots of **(I)** and **(II)** were generated using the *CrystalExplorer* software (Version 3.1; Wolff *et al.*, 2013), and the corresponding CIFs were used as the input files (Figs. 8 and 9). In the HS of **(I)**, the  $\text{N}-\text{H}\cdots\text{O}=\text{P}$  and  $\text{C}-\text{H}\cdots\text{O}=\text{P}$  hydrogen bonds appear as large (label **1**) and small (label **2**) red areas (Fig. 8*a*), and in the HS of **(II)**, the small and pale-red areas are related to  $\text{C}-\text{H}\cdots\pi$  interactions (Fig. 9*a*). It should be noted that in the HS maps, the contacts shown in red highlight intermolecular interactions with distances shorter than the sum of the van der Waals radii (McKinnon *et al.*, 2007).

Figs. 8(*b*)–(*i*) and 9(*b*)–(*i*) illustrate the FPs for **(I)** and **(II)**, respectively. For both structures, the  $\text{H}\cdots\text{H}$  contacts represent

the largest relative contribution [66.3% for **(I)** (Fig. 8*f*) and 58.4% for **(II)** (Fig. 9*f*)], with one sharp spike for structure **(I)** (the shortest  $d_e = d_i \approx 1.1$  Å). The other interactions are  $\text{O}\cdots\text{H}/\text{H}\cdots\text{O}$ ,  $\text{C}\cdots\text{H}/\text{H}\cdots\text{C}$  and  $\text{C}\cdots\text{C}$  for both structures, and  $\text{O}\cdots\text{C}/\text{C}\cdots\text{O}$  and  $\text{N}\cdots\text{H}/\text{H}\cdots\text{N}$  for **(II)**, with the percentages of contributions as given in the figures. It should be noted that the relatively large contribution of the  $\text{C}\cdots\text{H}/\text{H}\cdots\text{C}$  contacts (32.3%) (Fig. 9*g*) in **(II)** is a result of the presence of  $\text{C}-\text{H}\cdots\pi$  interactions.

**3.3.2. Energy frameworks.** In order to better understand the crystal packing and visualize the interaction topologies of **(I)** and **(II)**, an energy framework analysis was carried out using *CrystalExplorer* software (Thomas *et al.*, 2018). The electrostatic, polarization, dispersion and exchange–repulsion energies of the interactions between the molecules are calculated for **(I)** (Fig. 10 and Table S5 in the supporting information) and **(II)** (Fig. 11 and Table S6 in the supporting information) using B3LYP/6-31G(d,p) electron-density functions. The energies between molecular pairs are represented as cylinders (scale size of 150) by joining the centroids of pairs of molecules. The energy frameworks for  $E_{\text{ele}}$  (Figs. 10*d*–*f*),  $E_{\text{disp}}$  (Figs. 10*g*–*i*) and  $E_{\text{tot}}$  (Figs. 10*j*–*l*) are shown in red, green and blue, respectively, for **(I)**. Similarly, the energy frameworks for  $E_{\text{ele}}$  (Figs. 11*d*–*f*),  $E_{\text{disp}}$  (Figs. 11*g*–*i*) and  $E_{\text{tot}}$  (Figs. 11*j*–*l*) are

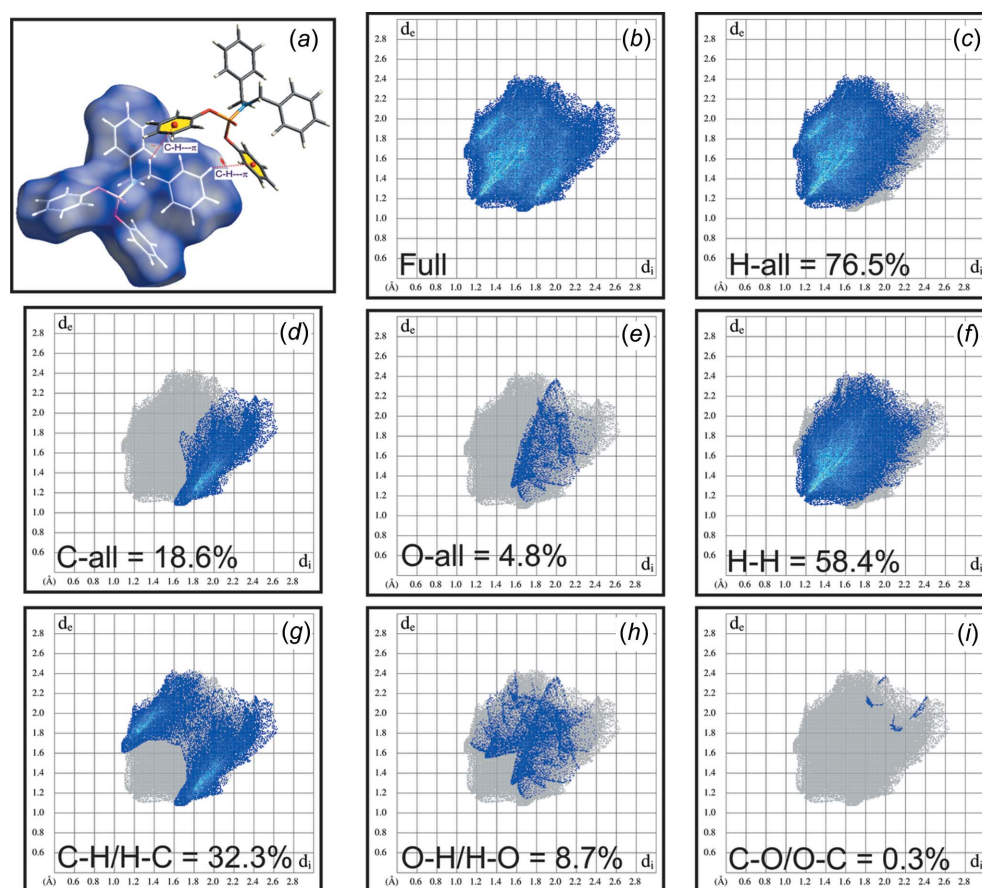


**Figure 9**

(*a*) The  $d_{\text{norm}}$ -mapped Hirshfeld surface for visualizing the  $\text{C}-\text{H}\cdots\pi$  interactions in the structure of **(II)**. 2D fingerprint plots of **(II)** for (*b*) full, (*c*)  $\text{H}\cdots\text{All}$ , (*d*)  $\text{C}\cdots\text{All}$ , (*e*)  $\text{O}\cdots\text{All}$ , (*f*)  $\text{H}\cdots\text{H}$ , (*g*)  $\text{C}\cdots\text{H}/\text{H}\cdots\text{C}$ , (*h*)  $\text{O}\cdots\text{H}/\text{H}\cdots\text{O}$  and (*i*)  $\text{O}\cdots\text{C}/\text{C}\cdots\text{O}$ . The  $\text{C}\cdots\text{C}$  (0.2%),  $\text{N}\cdots\text{all}$  (0.1%),  $\text{N}\cdots\text{H}/\text{H}\cdots\text{N}$  (0.1%) and  $\text{P}\cdots\text{All}$  (0%) are not shown.

shown for **(II)**. The largest pairwise energies calculated are  $-89.9$  (Table S5 in the supporting information) and  $-47.3$   $\text{kJ mol}^{-1}$  (Table S6 in the supporting information) for **(I)** and **(II)**, respectively. In both structures, the energy distribution patterns are different. The energy frameworks for **(I)** form zigzag molecular sheets and for **(II)** form parallel sheets. However, the dispersion energies outweigh the electrostatic energies in all cases. In general, **(I)** has higher electrostatic energies than **(II)**, which is visually evident from Figs. 10 and 11, and the 3D network topologies confirmed the significant contribution of the  $\text{N-H}\cdots\text{O}$  and  $\text{C-H}\cdots\text{O}$

interactions in **(I)**, and the  $\text{C-H}\cdots\pi$  interactions in **(II)**. It should be noted that the energies can be affected by conformational changes, similar to what was observed for the relationship of the  $\text{C}_6\text{H}_5\text{O}$  segments in **(I)** and **(II)**, which show the absence of  $\text{C-H}\cdots\pi$  interactions in **(I)** but their presence in **(II)**.

### 3.4. CSD data set

176 structures containing the  $\text{P(O)(OPh)}_2\text{N}$  skeleton were extracted from the CSD. Of these structures, 58 were rejected due to the non-availability of 3D coordinates, disordered

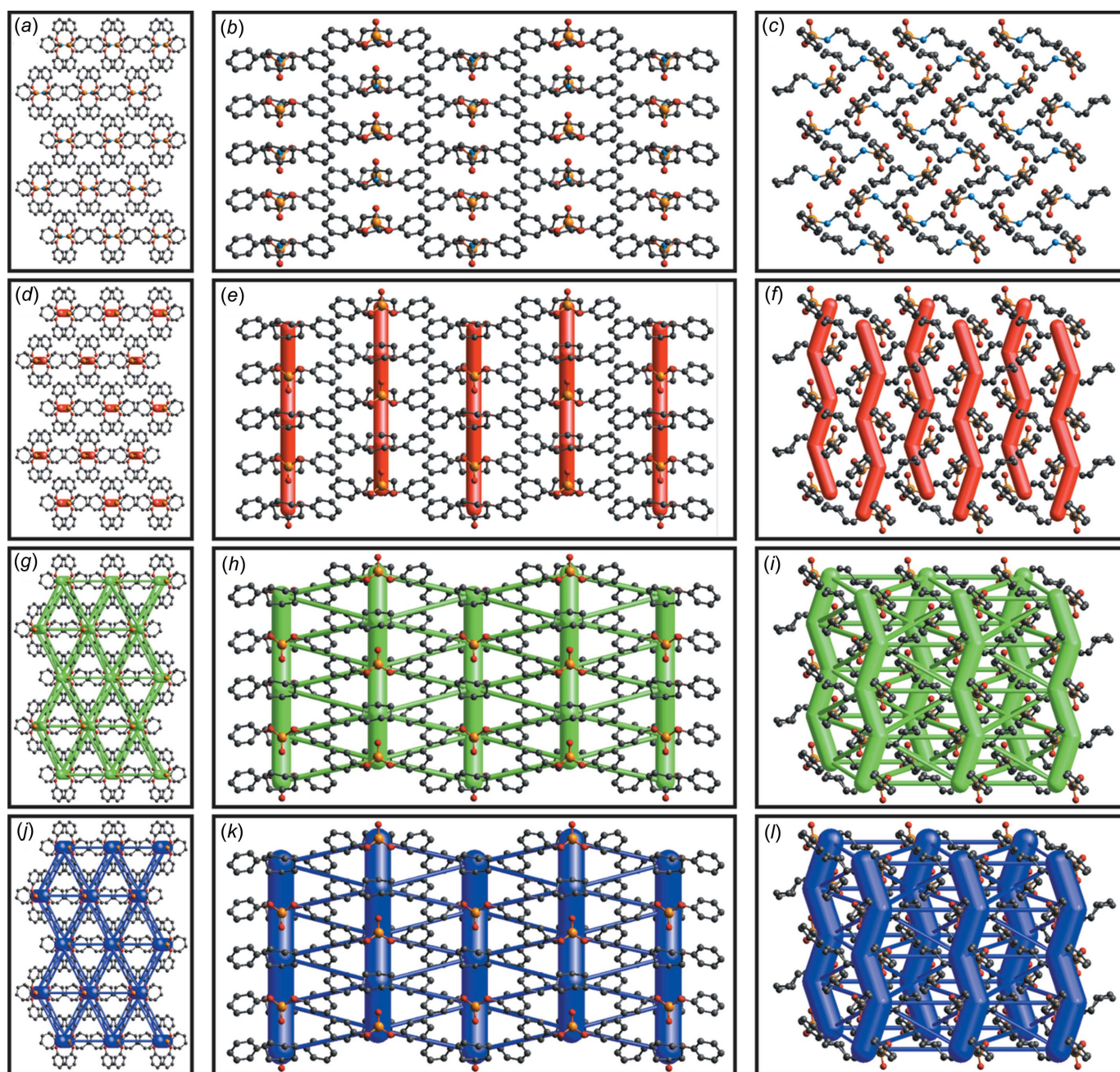
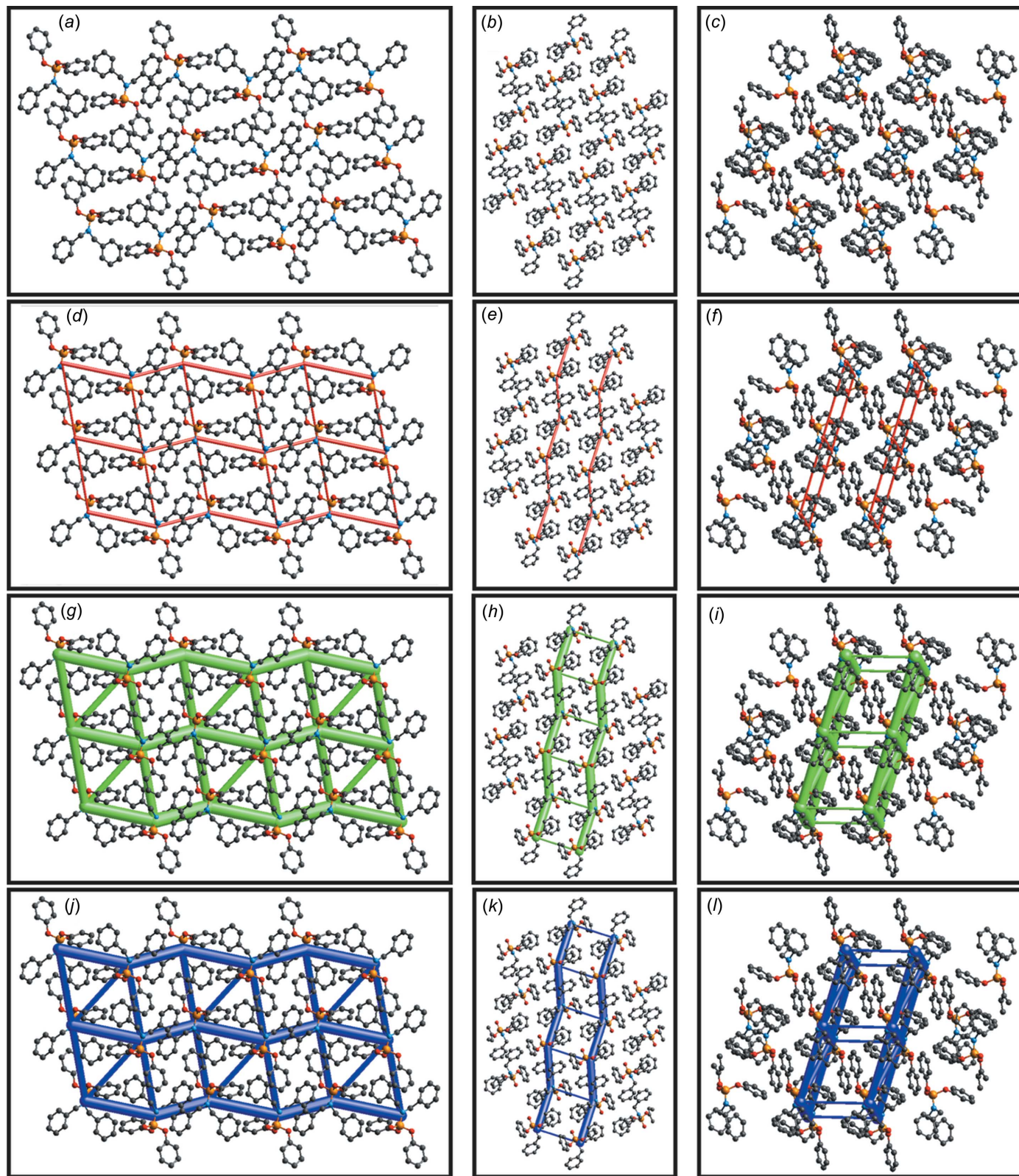


Figure 10

Energy frameworks for **(I)**. The molecular arrangement of **(I)** viewed along (a) the *a*, (b) the *b* and (c) the *c* directions, and shown as ball-and-stick models. (d)–(f) Representations of the electrostatic term (red colour), (g)–(i) the dispersion term (green colour) and (j)–(l) the total interaction energy (blue colour). H atoms have been omitted for clarity.

phenyl rings or both phenyl rings being fused *via* a single bond or the P=O group fused to other moieties. In the remaining

118 structures, some contain more than one molecule in the asymmetric unit. In total, 162 molecules from the 118 CSD



**Figure 11**  
 Energy frameworks for (II). The molecular arrangement of (II) viewed along (a) the *a*, (b) the *b* and (c) the *c* directions, and shown as ball-and-stick models. (d)–(f) Representations of the electrostatic term (red colour), (g)–(i) the dispersion term (green colour) and (j)–(l) the total interaction energy (blue colour). H atoms have been omitted for clarity.

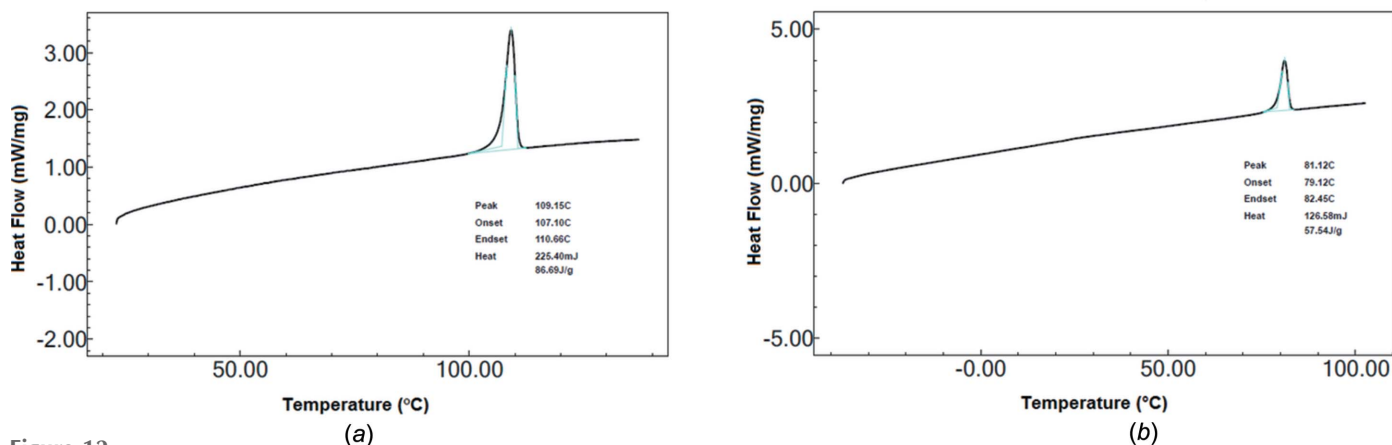


Figure 12 DSC curves of compounds (a) (**I**) and (b) (**II**). Both curves were obtained at a heating rate of  $10\text{ }^{\circ}\text{C min}^{-1}$  under an  $\text{N}_2$  atmosphere.

structures were used for a comparative study with the title compounds (**I**) and (**II**). The figures were rendered using *PyMOL* (Schrödinger, 2015).

### 3.5. DSC study

The thermal properties of the two title structures were studied by differential scanning calorimetry (DSC) analysis. The peaks in the DSC plots in Figs. 12(a) and 12(b) are at 109 and  $81\text{ }^{\circ}\text{C}$  for (**I**) and (**II**), respectively, and correspond to the melting of the compounds. The higher melting point of (**I**) can be directly correlated to the greater strength of the intermolecular contacts with respect to (**II**), as was discussed in the X-ray crystallography (§3.1) and energy framework (§3.3.2) sections. Furthermore, the thermal nature of the crystal is expected to be related to the flexibility of the molecule. The Hirshfeld rigid-bond test was also conducted for (**I**) and (**II**) (Hirshfeld, 1976) in order to understand the flexible natures of the structures. According to the rigid-bond test, the mean-squared displacement amplitudes do not show any significant bond deviation within  $5.0\sigma$  for both structures, except for three bonds of (**I**), namely P1—O2 ( $5.2\sigma$ ), C3—C4 ( $5.2\sigma$ ) and C11—C16 ( $6.0\sigma$ ), which show slight differences. In fact, this result is consistent with the CSD data, and these bond lengths vary slightly from the average obtained from the CSD data and the structure of (**II**) (Fig. 3a and Section §3.2.1). In any case, it is likely that there is conformational flexibility for these two structures and this is consistent with the CSD, Hirshfeld rigid-bond and energy framework studies.

### Acknowledgements

Support of this investigation by the Ferdowsi University of Mashhad is gratefully acknowledged. The authors appreciatively acknowledge the Cambridge Crystallographic Data Centre for access to the CSD Enterprise suite. A CIISB research infrastructure project funded by MEYS CR is gratefully acknowledged for the financial support of the measurements at the CF X-ray diffraction and Bio-SAXS. Abdul Ajees Abdul Salam acknowledges the research grant

provided by the Manipal Academy of Higher Education (MAHE), Manipal, India, under intramural funding.

### Funding information

Funding for this research was provided by: Ferdowsi University of Mashhad (project No. 39847/3); MEYS CR (project No. LM2015043); Manipal Academy of Higher Education (grant No. MAHE/DREG/PhD/IMF/2019).

### References

- Allcock, H. R., Ngo, D. C., Parvez, M. & Visscher, K. B. (1994). *Inorg. Chem.* **33**, 2090–2102.
- Ammon, H. L., El-Sayed, K. & Fouli, F. A. (1991). *Acta Cryst.* **C47**, 194–196.
- Aparna, K., Krishnamurthy, S. S. & Nethaji, M. (1995). *Z. Anorg. Allg. Chem.* **621**, 1913–1921.
- Attanasi, O. A., Filippone, P., Guerra, P., Serra-Zanetti, F., Foresti, E. & Tugnoli, V. (1988). *Gazz. Chim. Ital.* **118**, 533.
- Balakrishna, M. S., Santarsiero, B. D. & Cavell, R. G. (1994). *Inorg. Chem.* **33**, 3079–3084.
- Bernstein, J., Davis, R. E., Shimoni, L. & Chang, N.-L. (1995). *Angew. Chem. Int. Ed. Engl.* **34**, 1555–1573.
- Bernstein, J. & Hagler, A. T. (1978). *J. Am. Chem. Soc.* **100**, 673–681.
- Betteridge, P. W., Carruthers, J. R., Cooper, R. I., Prout, K. & Watkin, D. J. (2003). *J. Appl. Cryst.* **36**, 1487.
- Buntine, M. A., Hall, V. J., Kosovel, F. J. & Tiekink, E. R. T. (1998). *J. Phys. Chem. A*, **102**, 2472–2482.
- Cadierno, V., Díez, J., García-Álvarez, J. & Gimeno, J. (2004a). *Organometallics*, **23**, 3425–3436.
- Cadierno, V., Díez, J., García-Álvarez, J., Gimeno, J., Calhorda, M. J. & Veiros, L. F. (2004b). *Organometallics*, **23**, 2421–2433.
- Chandrasekaran, P., Mague, J. T. & Balakrishna, M. S. (2011). *Eur. J. Inorg. Chem.* **2011**, 2264–2272.
- Corbridge, D. E. C. (1995). In *Phosphorus: An Outline of Its Chemistry, Biochemistry and Technology*, 5th ed. Amsterdam: Elsevier.
- Das, D., Brahmmananda Rao, C. V. S., Sivaraman, N., Sivaramakrishna, A. & Vijayakrishna, K. (2018). *Inorg. Chim. Acta*, **482**, 597–604.
- Dauber, P. & Hagler, A. T. (1980). *Acc. Chem. Res.* **13**, 105–112.
- Drewelies, K. & Pritzkow, H. (1982). *Z. Naturforsch. B Chem. Sci.* **37**, 1402–1405.
- Du, D.-M., Hua, W.-T. & Jin, X.-L. (2001). *J. Mol. Struct.* **561**, 145–152.

- Endeshaw, M. M., Hansen, L. K. & Gautun, O. R. (2008). *J. Heterocycl. Chem.* **45**, 149–154.
- Fang, Z., Cao, C., Chen, J. & Deng, X. (2014). *J. Mol. Struct.* **1063**, 307–312.
- Flack, H. D. (1983). *Acta Cryst.* **A39**, 876–881.
- Gholivand, K. & Pourayoubi, M. (2004). *Z. Anorg. Allg. Chem.* **630**, 1330–1335.
- Gholivand, K., Shariatinia, Z. & Pourayoubi, M. (2005). *Z. Naturforsch. B Chem. Sci.* **60**, 67–74.
- Gholivand, K., Valmoozi, A. A. E. & Mahzouni, H. R. (2013). *Acta Cryst.* **B69**, 55–61.
- Gregoret, L. M. & Cohen, F. E. (1991). *J. Mol. Biol.* **219**, 109–122.
- Groom, C. R., Bruno, I. J., Lightfoot, M. P. & Ward, S. C. (2016). *Acta Cryst.* **B72**, 171–179.
- Gupta, A. K., Dubey, D. K., Sharma, M. & Kaushik, M. P. (2007). *Org. Prep. Proced. Int.* **39**, 297–305.
- Gupta, A. K., Palit, M., Dubey, D. K. & Raza, S. K. (2005). *Eur. J. Mass. Spectrom. (Chichester)*, **11**, 119–125.
- Herrmann, E., Nouaman, M., Zak, Z., Grömann, G. & Ohms, G. (1994). *Z. Anorg. Allg. Chem.* **620**, 1879–1888.
- Hirshfeld, F. L. (1976). *Acta Cryst.* **A32**, 239–244.
- Hooft, R. W. W., Straver, L. H. & Spek, A. L. (2008). *J. Appl. Cryst.* **41**, 96–103.
- Hopfinger, A. J. & Battershell, R. D. (1976). *J. Med. Chem.* **19**, 569–573.
- Jones, C. S., Bull, S. D. & Williams, J. M. J. (2016). *Org. Biomol. Chem.* **14**, 8452–8456.
- Keikha, M., Pourayoubi, M., van der Lee, A. & Tarahhomi, A. (2017). *Z. Kristallogr.* **232**, 3–13.
- Krishna, H., Krishnamurthy, S. S., Nethaji, M., Murugavel, R. & Prabusankar, G. (2007). *Dalton Trans.* pp. 2908–2914.
- Lee, A. van der (2013). *J. Appl. Cryst.* **46**, 1306–1315.
- Mattern, R. H., Moore, S. B., Tran, T. A., Rueter, J. K. & Goodman, M. (2000). *Tetrahedron*, **56**, 9819–9831.
- McKinnon, J. J., Jayatilaka, D. & Spackman, M. A. (2007). *Chem. Commun.* pp. 3814–3816.
- Moghaddam, S. N., Shabari, A. R., Sabbaghi, F., Pourayoubi, M. & Salam, A. A. A. (2019). *Molbank*, **2019**, M1051.
- Necas, M., Foreman, M. R. St J., Marek, J., Derek Woollins, J. & Novosad, J. (2001). *New J. Chem.* **25**, 1256–1263.
- Palatinus, L. & Chapuis, G. (2007). *J. Appl. Cryst.* **40**, 786–790.
- Rebrova, O. N., Biyushkin, V. I., Ovrutskii, V. M., Nezhel'skaya, L. A., Dneprova, T. N. & Malinovskii, T. I. (1993). *Kristallografiya*, **38**, 276.
- Richter, R., Sieler, J., Borrmann, H., Simon, A., Chau, N. T. T. & Herrmann, E. (1991). *Phosphorus Sulfur Silicon*, **60**, 107–117.
- Rigaku (2011). *CrystalClear-SM Expert*. Rigaku Americas Corporation, The Woodlands, Texas, USA.
- Rigaku OD (2015). *CrysAlis PRO*. Rigaku Oxford Diffraction Ltd, Yarnton, Oxfordshire, England.
- Rollet, J. S. (1965). Editor. *Computing Methods in Crystallography*, 1st ed., p. 170. Oxford: Pergamon Press.
- Rybarczyk-Pirek, A. J., Grabowski, S. J., Małecka, M. & Nawrot-Modranka, J. (2002a). *J. Phys. Chem. A*, **106**, 11956–11962.
- Rybarczyk-Pirek, A. J., Małecka, M., Grabowski, S. J. & Nawrot-Modranka, J. (2002b). *Acta Cryst.* **C58**, o405–o406.
- Sabbaghi, F., Pourayoubi, M., Dušek, M., Eigner, V., Bayat, S., Damodaran, K., Nečas, M. & Kučeráková, M. (2016). *Struct. Chem.* **27**, 1831–1844.
- Sabbaghi, F., Pourayoubi, M., Nečas, M. & Damodaran, K. (2019). *Acta Cryst.* **C75**, 77–84.
- Sabbaghi, F., Pourayoubi, M. & Zargaran, P. (2011a). *Acta Cryst.* **E67**, o1170.
- Sabbaghi, F., Pourayoubi, M., Zargaran, P., Bruno, G. & Amiri Rudbari, H. (2011b). *Acta Cryst.* **E67**, o1378.
- Safin, D. A., Babashkina, M. G., Robeyns, K., Mitoraj, M. P., Kubisiak, P., Brela, M. & Garcia, Y. (2013). *CrystEngComm*, **15**, 7845–7851.
- Schrödinger (2015). *The pyMOL Molecular Graphics System*. Open-Source Version 1.5.5. Schrödinger Inc., Portland, OR, USA.
- Sheldrick, G. M. (2015a). *Acta Cryst.* **A71**, 3–8.
- Sheldrick, G. M. (2015b). *Acta Cryst.* **C71**, 3–8.
- Simon, L., Abdol Salam, A. A., Madan Kumar, S., Shilpa, T., Srinivasan, K. K. & Byrappa, K. (2017). *Bioorg. Med. Chem. Lett.* **27**, 5284–5290.
- Thomas, S. P., Spackman, P. R., Jayatilaka, D. & Spackman, M. A. (2018). *J. Chem. Theory Comput.* **14**, 1614–1623.
- Toghraee, M., Pourayoubi, M. & Divjakovic, V. (2011). *Polyhedron*, **30**, 1680–1690.
- Vahdani Alviri, B., Pourayoubi, M., Saneei, A., Keikha, M., van der Lee, A., Crochet, A., Ajees, A. A., Nečas, M., Fromm, K. M., Damodaran, K. & Jenny, T. A. (2018). *Tetrahedron*, **74**, 28–41.
- Warren, T. K., *et al.* (2016). *Nature*, **531**, 381–385.
- Waser, J. (1963). *Acta Cryst.* **16**, 1091–1094.
- Watkin, D. J., Prout, C. K. & Pearce, L. J. (1996). *CAMERON*. Chemical Crystallography Laboratory, Oxford, England.
- Wolff, S. K., Grimwood, D. J., McKinnon, J. J., Turner, M. J., Jayatilaka, D. & Spackman, M. A. (2013). *CrystalExplorer*. The University of Western Australia. <http://crystalexplorer.scb.uwa.edu.au/>.
- Zák, Z., Fofana, M., Kameníček, J. & Glowiak, T. (1989). *Acta Cryst.* **C45**, 1686–1689.

## supporting information

*Acta Cryst.* (2020). C76, 104-116 [https://doi.org/10.1107/S2053229619016619]

## Conformational flexibility in amidophosphoesters: a CSD analysis completed with two new crystal structures of $(\text{C}_6\text{H}_5\text{O})_2\text{P}(\text{O})\text{X}$ [ $\text{X} = \text{NHC}_7\text{H}_{13}$ and $\text{N}(\text{CH}_2\text{C}_6\text{H}_5)_2$ ]

**Banafsheh Vahdani Alviri, Mehrdad Pourayoubi, Abdul Ajees Abdul Salam, Marek Nečas, Arie van der Lee, Akshara Chithran and Krishnan Damodaran**

### Computing details

Data collection: *CrysAlis PRO* (Rigaku OD, 2015) for (I); Rigaku *CrystalClear-SM Expert* (Rigaku, 2011) for (II). For both structures, cell refinement: *CrysAlis PRO* (Rigaku OD, 2015); data reduction: *CrysAlis PRO* (Rigaku OD, 2015). Program(s) used to solve structure: SUPERFLIP (Palatinus & Chapuis, 2007) for (I); SHELXT2014 (Sheldrick, 2015a) for (II). Program(s) used to refine structure: *CRYSTALS* (Betteridge *et al.*, 2003) for (I); *SHELXL2018* (Sheldrick, 2015b) for (II). For both structures, molecular graphics: *CAMERON* (Watkin *et al.*, 1996) and *pyMOL* (Schrödinger, 2015). Software used to prepare material for publication: *CRYSTALS* (Betteridge *et al.*, 2003) for (I); *SHELXL2018* (Sheldrick, 2015b) for (II).

### Diphenyl (cycloheptylamido)phosphate (I)

#### Crystal data

$\text{C}_{19}\text{H}_{24}\text{NO}_3\text{P}$

$M_r = 345.36$

Orthorhombic, *Pna*2<sub>1</sub>

Hall symbol: P 2c -2n

$a = 9.3538$  (2) Å

$b = 9.7899$  (3) Å

$c = 19.3432$  (5) Å

$V = 1771.31$  (5) Å<sup>3</sup>

$Z = 4$

$F(000) = 736$

$D_x = 1.295$  Mg m<sup>-3</sup>

Mo  $K\alpha$  radiation,  $\lambda = 0.71073$  Å

Cell parameters from 3874 reflections

$\theta = 2.1\text{--}27.1^\circ$

$\mu = 0.17$  mm<sup>-1</sup>

$T = 175$  K

Prism, colourless

$0.35 \times 0.25 \times 0.15$  mm

#### Data collection

Rigaku Xcalibur Sapphire3 Gemini  
diffractometer

Graphite monochromator

Detector resolution: 16.0143 pixels mm<sup>-1</sup>

$\omega$  scans

Absorption correction: multi-scan  
(*CrysAlis PRO*; Rigaku OD, 2015)

$T_{\min} = 0.979$ ,  $T_{\max} = 1.000$

9026 measured reflections

3411 independent reflections

2964 reflections with  $I > 2.0\sigma(I)$

$R_{\text{int}} = 0.035$

$\theta_{\max} = 28.0^\circ$ ,  $\theta_{\min} = 2.1^\circ$

$h = -7 \rightarrow 12$

$k = -9 \rightarrow 11$

$l = -23 \rightarrow 23$

Refinement

Refinement on  $F^2$   
 Least-squares matrix: full  
 $R[F^2 > 2\sigma(F^2)] = 0.052$   
 $wR(F^2) = 0.103$   
 $S = 0.95$   
 3338 reflections  
 221 parameters  
 79 restraints  
 Primary atom site location: iterative  
 Hydrogen site location: difference Fourier map  
 H atoms treated by a mixture of independent  
 and constrained refinement

Method, part 1, Chebychev polynomial,  
 (Watkin, 1994, Prince, 1982) [weight] =  
 $1.0/[A_0*T_0(x) + A_1*T_1(x) \dots + A_{n-1}*T_{n-1}(x)]$   
 where  $A_i$  are the Chebychev coefficients listed  
 below and  $x = F/F_{max}$  Method = Robust  
 Weighting (Prince, 1982)  $W = [weight]^*$   
 $[1-(\Delta F/6*\sigma F)^2]^2$   $A_i$  are: 19.6 25.7 7.98  
 $(\Delta/\sigma)_{max} = 0.001$   
 $\Delta\rho_{max} = 0.32 \text{ e } \text{\AA}^{-3}$   
 $\Delta\rho_{min} = -0.54 \text{ e } \text{\AA}^{-3}$   
 Absolute structure: Flack (1983), 1505 Friedel-  
 pairs  
 Absolute structure parameter: 0.6 (3)

Special details

**Experimental.** The crystal was placed in the cold stream of an Oxford Cryosystems open-flow nitrogen cryostat (Cosier & Glazer, 1986) with a nominal stability of 0.1K.

Cosier, J. & Glazer, A.M., 1986. *J. Appl. Cryst.* 105-107.

**Refinement.** Data collection and crystal screening for **(I)** was performed on a Rigaku Oxford-Diffraction Gemini-S diffractometer with sealed-tube Mo- $K\alpha$  radiation using the *CrysAlisPro* program (Rigaku Oxford-Diffraction, 2012). This program was also used for the integration of the data using default parameters, for the empirical absorption correction using spherical harmonics employing symmetry-equivalent and redundant data, and the correction for Lorentz and polarization effects. The *ab-initio* iterative charge flipping method was used to solve the crystal structure of **(I)** with parameters described elsewhere (van der Lee, 2013) employing the *Superflip* program (Palatinus&Chapuis, 2007) and it was refined using full-matrix least-squares procedures on squared structure factor amplitudes  $F^2$  as implemented in *CRYSTALS* (Betteridge *et al.*, 2003) using all independent reflections with  $I > 0$ .

Fractional atomic coordinates and isotropic or equivalent isotropic displacement parameters ( $\text{\AA}^2$ )

	x	y	z	$U_{iso}^*/U_{eq}$
P1	0.35676 (6)	0.84662 (6)	0.00163 (13)	0.0183
O2	0.4415 (4)	0.9225 (3)	0.06247 (18)	0.0205
C3	0.4113 (6)	0.8932 (5)	0.1321 (3)	0.0257
C4	0.4887 (6)	0.7907 (5)	0.1653 (2)	0.0305
C5	0.4633 (8)	0.7722 (6)	0.2345 (3)	0.0433
C6	0.3634 (7)	0.8486 (7)	0.2706 (3)	0.0431
C7	0.2905 (8)	0.9495 (7)	0.2365 (3)	0.0406
C8	0.3173 (7)	0.9711 (6)	0.1665 (3)	0.0333
H81	0.2689	1.0405	0.1435	0.0500*
H71	0.2237	1.0015	0.2605	0.0500*
H61	0.3472	0.8316	0.3172	0.0500*
H51	0.5151	0.7058	0.2580	0.0500*
H41	0.5550	0.7374	0.1417	0.0500*
O9	0.20228 (18)	0.87095 (18)	0.0010 (3)	0.0275
O10	0.4444 (4)	0.9209 (4)	-0.0573 (2)	0.0288
C11	0.4140 (5)	0.8929 (5)	-0.1266 (3)	0.0223
C12	0.3098 (6)	0.9729 (6)	-0.1603 (3)	0.0323
C13	0.2900 (8)	0.9499 (8)	-0.2298 (3)	0.0459
C14	0.3672 (7)	0.8504 (7)	-0.2635 (4)	0.0488
C15	0.4657 (7)	0.7703 (7)	-0.2302 (3)	0.0420

C16	0.4909 (7)	0.7958 (6)	-0.1596 (2)	0.0358
H161	0.5592	0.7455	-0.1357	0.0500*
H151	0.5141	0.7017	-0.2538	0.0500*
H141	0.3519	0.8376	-0.3106	0.0500*
H131	0.2239	1.0023	-0.2540	0.0500*
N17	0.3982 (2)	0.6874 (2)	0.0026 (3)	0.0213
C18	0.2936 (3)	0.5742 (2)	0.0018 (3)	0.0232
C19	0.3086 (7)	0.4933 (6)	0.0682 (3)	0.0425
C20	0.4369 (7)	0.3947 (6)	0.0702 (3)	0.0671
C21	0.4344 (6)	0.2720 (4)	0.0185 (3)	0.0809
C22	0.4727 (8)	0.2979 (6)	-0.0558 (3)	0.0828
C23	0.4388 (6)	0.4358 (5)	-0.0842 (3)	0.0460
C24	0.2980 (6)	0.4913 (5)	-0.0638 (3)	0.0330
H241	0.2705	0.5513	-0.1015	0.0500*
H242	0.2268	0.4196	-0.0609	0.0500*
H231	0.4456	0.4317	-0.1342	0.0500*
H232	0.5135	0.4971	-0.0684	0.0500*
H191	0.2225	0.4394	0.0742	0.0500*
H192	0.3146	0.5558	0.1070	0.0500*
H181	0.1988	0.6165	0.0040	0.0500*
H201	0.5191	0.4478	0.0598	0.0830*
H202	0.4452	0.3584	0.1155	0.0830*
H211	0.4991	0.2058	0.0360	0.1300*
H212	0.3399	0.2364	0.0198	0.1300*
H221	0.5721	0.2813	-0.0614	0.1047*
H222	0.4199	0.2331	-0.0820	0.1047*
H121	0.2592	1.0429	-0.1367	0.0436*
H171	0.484 (2)	0.6673 (19)	-0.009 (2)	0.0300*

Atomic displacement parameters ( $\text{\AA}^2$ )

	$U^{11}$	$U^{22}$	$U^{33}$	$U^{12}$	$U^{13}$	$U^{23}$
P1	0.0138 (3)	0.0183 (3)	0.0227 (3)	-0.0001 (2)	0.0006 (7)	-0.0007 (6)
O2	0.0227 (17)	0.0164 (13)	0.0223 (15)	-0.0076 (15)	-0.0063 (14)	-0.0020 (13)
C3	0.029 (3)	0.028 (2)	0.020 (2)	-0.011 (2)	0.002 (2)	-0.007 (2)
C4	0.029 (3)	0.024 (2)	0.039 (3)	0.008 (2)	-0.011 (2)	-0.003 (2)
C5	0.055 (5)	0.042 (3)	0.033 (3)	0.005 (3)	-0.014 (3)	0.002 (3)
C6	0.058 (5)	0.055 (4)	0.016 (3)	-0.018 (3)	0.004 (3)	0.003 (2)
C7	0.045 (4)	0.044 (3)	0.033 (3)	0.005 (3)	0.018 (3)	-0.015 (3)
C8	0.037 (3)	0.034 (3)	0.029 (3)	0.006 (2)	0.010 (2)	-0.007 (2)
O9	0.0155 (8)	0.0237 (9)	0.0434 (11)	0.0019 (7)	-0.004 (2)	-0.006 (2)
O10	0.027 (2)	0.0371 (17)	0.0223 (15)	-0.0064 (19)	-0.0090 (16)	0.0040 (15)
C11	0.016 (3)	0.026 (2)	0.025 (2)	-0.003 (2)	0.002 (2)	0.003 (2)
C12	0.023 (3)	0.034 (3)	0.040 (3)	-0.003 (2)	0.003 (2)	0.005 (3)
C13	0.038 (4)	0.058 (4)	0.042 (3)	-0.011 (4)	-0.011 (3)	0.012 (3)
C14	0.043 (5)	0.069 (5)	0.034 (4)	-0.011 (3)	-0.009 (3)	0.015 (3)
C15	0.039 (4)	0.055 (4)	0.032 (3)	-0.008 (3)	0.005 (3)	-0.010 (3)
C16	0.036 (3)	0.052 (3)	0.020 (3)	-0.004 (3)	-0.008 (2)	0.004 (2)

N17	0.0128 (9)	0.0206 (10)	0.0305 (12)	0.0018 (8)	0.003 (3)	-0.006 (2)
C18	0.0189 (12)	0.0192 (12)	0.0316 (13)	-0.0034 (10)	0.008 (2)	0.001 (2)
C19	0.057 (3)	0.040 (2)	0.030 (2)	-0.018 (2)	0.011 (3)	0.007 (2)
C20	0.056 (3)	0.071 (3)	0.074 (3)	-0.007 (3)	-0.019 (3)	0.047 (2)
C21	0.058 (3)	0.0235 (17)	0.161 (4)	0.0095 (18)	0.021 (4)	0.037 (2)
C22	0.065 (4)	0.052 (2)	0.131 (4)	0.018 (3)	0.001 (3)	-0.013 (2)
C23	0.039 (2)	0.053 (2)	0.046 (2)	0.002 (2)	-0.002 (2)	-0.0226 (17)
C24	0.029 (2)	0.036 (2)	0.034 (2)	-0.006 (2)	-0.001 (2)	-0.0073 (19)

*Geometric parameters (Å, °)*

P1—O2	1.601 (3)	C15—C16	1.409 (6)
P1—O9	1.4645 (18)	C15—H151	0.930
P1—O10	1.581 (4)	C16—H161	0.930
P1—N17	1.607 (2)	N17—C18	1.479 (3)
O2—C3	1.405 (6)	N17—H171	0.860 (18)
C3—C4	1.394 (6)	C18—C19	1.514 (6)
C3—C8	1.341 (7)	C18—C24	1.507 (6)
C4—C5	1.371 (6)	C18—H181	0.980
C4—H41	0.930	C19—C20	1.540 (7)
C5—C6	1.385 (7)	C19—H191	0.970
C5—H51	0.930	C19—H192	0.970
C6—C7	1.369 (7)	C20—C21	1.563 (6)
C6—H61	0.930	C20—H201	0.950
C7—C8	1.394 (6)	C20—H202	0.950
C7—H71	0.930	C21—C22	1.502 (7)
C8—H81	0.930	C21—H211	0.950
O10—C11	1.399 (6)	C21—H212	0.950
C11—C12	1.409 (6)	C22—C23	1.491 (6)
C11—C16	1.351 (7)	C22—H221	0.950
C12—C13	1.377 (6)	C22—H222	0.950
C12—H121	0.950	C23—C24	1.478 (6)
C13—C14	1.377 (7)	C23—H231	0.970
C13—H131	0.930	C23—H232	0.970
C14—C15	1.370 (7)	C24—H241	0.970
C14—H141	0.930	C24—H242	0.970
O2—P1—O9	114.8 (3)	P1—N17—H171	116.4 (13)
O2—P1—O10	93.42 (10)	C18—N17—H171	116.5 (13)
O9—P1—O10	115.5 (3)	N17—C18—C19	108.8 (4)
O2—P1—N17	108.8 (2)	N17—C18—C24	113.2 (4)
O9—P1—N17	113.34 (11)	C19—C18—C24	115.5 (2)
O10—P1—N17	109.2 (2)	N17—C18—H181	106.4
P1—O2—C3	120.7 (3)	C19—C18—H181	105.6
O2—C3—C4	118.9 (5)	C24—C18—H181	106.8
O2—C3—C8	119.4 (5)	C18—C19—C20	114.9 (5)
C4—C3—C8	121.4 (5)	C18—C19—H191	108.0
C3—C4—C5	117.0 (5)	C20—C19—H191	107.6

C3—C4—H41	121.7	C18—C19—H192	109.3
C5—C4—H41	121.3	C20—C19—H192	109.3
C4—C5—C6	122.5 (6)	H191—C19—H192	107.4
C4—C5—H51	118.6	C19—C20—C21	117.0 (5)
C6—C5—H51	118.8	C19—C20—H201	106.3
C5—C6—C7	118.9 (6)	C21—C20—H201	107.4
C5—C6—H61	120.2	C19—C20—H202	108.8
C7—C6—H61	120.9	C21—C20—H202	107.8
C6—C7—C8	119.2 (6)	H201—C20—H202	109.5
C6—C7—H71	119.4	C20—C21—C22	118.6 (4)
C8—C7—H71	121.4	C20—C21—H211	106.6
C7—C8—C3	120.9 (6)	C22—C21—H211	107.8
C7—C8—H81	119.3	C20—C21—H212	106.2
C3—C8—H81	119.8	C22—C21—H212	108.0
P1—O10—C11	119.7 (3)	H211—C21—H212	109.5
O10—C11—C12	118.3 (5)	C21—C22—C23	117.0 (5)
O10—C11—C16	118.8 (5)	C21—C22—H221	108.2
C12—C11—C16	122.8 (5)	C23—C22—H221	108.7
C11—C12—C13	116.9 (6)	C21—C22—H222	105.8
C11—C12—H121	121.6	C23—C22—H222	107.4
C13—C12—H121	121.4	H221—C22—H222	109.5
C12—C13—C14	120.5 (7)	C22—C23—C24	115.1 (5)
C12—C13—H131	119.4	C22—C23—H231	108.4
C14—C13—H131	120.1	C24—C23—H231	109.8
C13—C14—C15	122.4 (7)	C22—C23—H232	106.9
C13—C14—H141	118.5	C24—C23—H232	109.3
C15—C14—H141	119.1	H231—C23—H232	107.1
C14—C15—C16	117.8 (6)	C18—C24—C23	116.5 (4)
C14—C15—H151	120.6	C18—C24—H241	107.4
C16—C15—H151	121.6	C23—C24—H241	105.0
C15—C16—C11	119.6 (6)	C18—C24—H242	108.8
C15—C16—H161	120.2	C23—C24—H242	111.2
C11—C16—H161	120.2	H241—C24—H242	107.4
P1—N17—C18	124.57 (17)		

Hydrogen-bond geometry (Å, °)

<i>D</i> —H... <i>A</i>	<i>D</i> —H	H... <i>A</i>	<i>D</i> ... <i>A</i>	<i>D</i> —H... <i>A</i>
C23—H232...O9 <sup>i</sup>	0.97	2.57	3.516 (8)	166 (1)
N17—H171...O9 <sup>i</sup>	0.86	2.08	2.901 (8)	159 (4)

Symmetry code: (i)  $x+1/2, -y+3/2, z$ .

Diphenyl (dibenzylamido)phosphate (II)

Crystal data

$C_{26}H_{24}NO_3P$   
 $M_r = 429.43$   
 Triclinic,  $P\bar{1}$

$a = 8.3404$  (3) Å  
 $b = 9.5349$  (5) Å  
 $c = 14.9677$  (7) Å

$\alpha = 76.280 (4)^\circ$   
 $\beta = 75.778 (4)^\circ$   
 $\gamma = 72.055 (4)^\circ$   
 $V = 1080.73 (9) \text{ \AA}^3$   
 $Z = 2$   
 $F(000) = 452$   
 $D_x = 1.320 \text{ Mg m}^{-3}$

Mo  $K\alpha$  radiation,  $\lambda = 0.71073 \text{ \AA}$   
 Cell parameters from 7627 reflections  
 $\theta = 3.7\text{--}29.8^\circ$   
 $\mu = 0.16 \text{ mm}^{-1}$   
 $T = 120 \text{ K}$   
 Block, colourless  
 $0.25 \times 0.20 \times 0.20 \text{ mm}$

*Data collection*

AFC11 (Right): Eulerian 3 circle CCD diffractometer  
 Radiation source: Rotating Anode MicroMax-007HF DW 1.2 kW  
 Profile data from  $\omega$ -scans  
 Absorption correction: multi-scan CrysAlis PRO (Rigaku OD, 2015)  
 $T_{\min} = 0.722$ ,  $T_{\max} = 1.000$

9523 measured reflections  
 3901 independent reflections  
 3578 reflections with  $I > 2\sigma(I)$   
 $R_{\text{int}} = 0.018$   
 $\theta_{\max} = 25.4^\circ$ ,  $\theta_{\min} = 3.2^\circ$   
 $h = -10 \rightarrow 10$   
 $k = -11 \rightarrow 11$   
 $l = -18 \rightarrow 18$

*Refinement*

Refinement on  $F^2$   
 Least-squares matrix: full  
 $R[F^2 > 2\sigma(F^2)] = 0.033$   
 $wR(F^2) = 0.086$   
 $S = 1.05$   
 3901 reflections  
 280 parameters  
 0 restraints

Hydrogen site location: inferred from neighbouring sites  
 H-atom parameters constrained  
 $w = 1/[\sigma^2(F_o^2) + (0.0421P)^2 + 0.4112P]$   
 where  $P = (F_o^2 + 2F_c^2)/3$   
 $(\Delta/\sigma)_{\max} = 0.021$   
 $\Delta\rho_{\max} = 0.27 \text{ e \AA}^{-3}$   
 $\Delta\rho_{\min} = -0.34 \text{ e \AA}^{-3}$

*Special details*

**Geometry.** All esds (except the esd in the dihedral angle between two l.s. planes) are estimated using the full covariance matrix. The cell esds are taken into account individually in the estimation of esds in distances, angles and torsion angles; correlations between esds in cell parameters are only used when they are defined by crystal symmetry. An approximate (isotropic) treatment of cell esds is used for estimating esds involving l.s. planes.

**Refinement.** Data collection and crystal screening for **(I)** was performed on a Rigaku Oxford-Diffraction Gemini-S diffractometer with sealed-tube Mo- $K\alpha$  radiation using the *CrysAlisPro* program (Rigaku Oxford-Diffraction, 2012). This program was also used for the integration of the data using default parameters, for the empirical absorption correction using spherical harmonics employing symmetry-equivalent and redundant data, and the correction for Lorentz and polarization effects. The *ab-initio* iterative charge flipping method was used to solve the crystal structure of **(I)** with parameters described elsewhere (van der Lee, 2013) employing the *Superflip* program (Palatinus&Chapuis, 2007) and it was refined using full-matrix least-squares procedures on squared structure factor amplitudes  $F^2$  as implemented in *CRYSTALS* (Betteridge *et al.*, 2003) using all independent reflections with  $I > 0$ .

*Fractional atomic coordinates and isotropic or equivalent isotropic displacement parameters ( $\text{\AA}^2$ )*

	<i>x</i>	<i>y</i>	<i>z</i>	$U_{\text{iso}}^*/U_{\text{eq}}$
P1	0.28992 (4)	0.22585 (4)	0.24553 (2)	0.02034 (11)
O1	0.19646 (12)	0.25264 (11)	0.16998 (7)	0.0268 (2)
O2	0.18570 (12)	0.30054 (10)	0.33444 (6)	0.0242 (2)
O3	0.44766 (12)	0.29786 (10)	0.22264 (6)	0.0229 (2)
N1	0.35880 (14)	0.04977 (12)	0.28829 (7)	0.0210 (2)
C1	0.11701 (16)	0.45642 (14)	0.32925 (9)	0.0216 (3)
C2	0.13891 (17)	0.51758 (16)	0.39864 (9)	0.0251 (3)
H2A	0.204474	0.457320	0.444418	0.030*

---

C3	0.06359 (18)	0.66858 (16)	0.40047 (10)	0.0283 (3)
H3A	0.077787	0.712423	0.447789	0.034*
C4	-0.03204 (17)	0.75573 (15)	0.33386 (10)	0.0279 (3)
H4A	-0.083810	0.859051	0.335667	0.033*
C5	-0.05239 (18)	0.69265 (16)	0.26462 (10)	0.0287 (3)
H5A	-0.117877	0.752952	0.218813	0.034*
C6	0.02249 (17)	0.54132 (15)	0.26162 (10)	0.0264 (3)
H6A	0.008991	0.497327	0.214182	0.032*
C7	0.58266 (16)	0.26177 (14)	0.14702 (9)	0.0212 (3)
C8	0.55543 (18)	0.31321 (15)	0.05655 (9)	0.0244 (3)
H8A	0.444962	0.369332	0.044181	0.029*
C9	0.69321 (19)	0.28115 (17)	-0.01621 (10)	0.0311 (3)
H9A	0.677120	0.314654	-0.079222	0.037*
C10	0.8537 (2)	0.2007 (2)	0.00263 (11)	0.0385 (4)
H10A	0.947575	0.179286	-0.047458	0.046*
C11	0.8781 (2)	0.1512 (2)	0.09426 (11)	0.0395 (4)
H11A	0.988814	0.096637	0.106884	0.047*
C12	0.74155 (18)	0.18102 (16)	0.16751 (10)	0.0287 (3)
H12A	0.756938	0.146579	0.230603	0.034*
C13	0.31490 (17)	-0.06607 (15)	0.25673 (9)	0.0241 (3)
H13A	0.224230	-0.017085	0.218789	0.029*
H13B	0.267326	-0.131358	0.312238	0.029*
C14	0.46539 (17)	-0.16227 (15)	0.19938 (9)	0.0227 (3)
C15	0.55410 (18)	-0.09884 (15)	0.11602 (10)	0.0256 (3)
H15A	0.524078	0.006721	0.096448	0.031*
C16	0.68566 (19)	-0.18823 (18)	0.06139 (11)	0.0334 (3)
H16A	0.744928	-0.144031	0.004279	0.040*
C17	0.7312 (2)	-0.34247 (19)	0.08992 (12)	0.0399 (4)
H17A	0.821881	-0.403902	0.052550	0.048*
C18	0.6445 (2)	-0.40617 (17)	0.17262 (13)	0.0389 (4)
H18A	0.675686	-0.511682	0.192324	0.047*
C19	0.5118 (2)	-0.31677 (15)	0.22719 (11)	0.0302 (3)
H19A	0.452266	-0.361485	0.284001	0.036*
C20	0.47160 (16)	-0.00427 (14)	0.35785 (9)	0.0215 (3)
H20A	0.491704	0.082604	0.374481	0.026*
H20B	0.583807	-0.065766	0.329936	0.026*
C21	0.39591 (16)	-0.09676 (14)	0.44588 (9)	0.0209 (3)
C22	0.48106 (18)	-0.24494 (16)	0.47433 (10)	0.0274 (3)
H22A	0.589320	-0.288210	0.439166	0.033*
C23	0.4090 (2)	-0.33073 (16)	0.55406 (11)	0.0327 (3)
H23A	0.468936	-0.431673	0.573441	0.039*
C24	0.2508 (2)	-0.26933 (17)	0.60496 (10)	0.0303 (3)
H24A	0.200719	-0.328244	0.658723	0.036*
C25	0.16556 (18)	-0.12152 (17)	0.57722 (10)	0.0281 (3)
H25A	0.056824	-0.078855	0.612209	0.034*
C26	0.23788 (17)	-0.03546 (15)	0.49876 (9)	0.0242 (3)
H26A	0.179122	0.066360	0.480840	0.029*

---

Atomic displacement parameters ( $\text{\AA}^2$ )

	$U^{11}$	$U^{22}$	$U^{33}$	$U^{12}$	$U^{13}$	$U^{23}$
P1	0.01953 (18)	0.02070 (19)	0.01905 (18)	-0.00377 (13)	-0.00332 (13)	-0.00256 (13)
O1	0.0258 (5)	0.0293 (5)	0.0242 (5)	-0.0051 (4)	-0.0080 (4)	-0.0022 (4)
O2	0.0241 (5)	0.0209 (5)	0.0218 (5)	-0.0006 (4)	-0.0015 (4)	-0.0026 (4)
O3	0.0243 (5)	0.0224 (5)	0.0217 (5)	-0.0070 (4)	-0.0007 (4)	-0.0062 (4)
N1	0.0220 (5)	0.0211 (6)	0.0214 (5)	-0.0054 (4)	-0.0068 (4)	-0.0039 (4)
C1	0.0166 (6)	0.0214 (6)	0.0229 (6)	-0.0039 (5)	0.0013 (5)	-0.0032 (5)
C2	0.0198 (6)	0.0310 (7)	0.0223 (7)	-0.0059 (5)	-0.0021 (5)	-0.0035 (6)
C3	0.0255 (7)	0.0319 (7)	0.0292 (7)	-0.0098 (6)	-0.0009 (6)	-0.0103 (6)
C4	0.0235 (7)	0.0232 (7)	0.0357 (8)	-0.0059 (5)	-0.0017 (6)	-0.0072 (6)
C5	0.0257 (7)	0.0253 (7)	0.0316 (8)	-0.0027 (6)	-0.0077 (6)	-0.0014 (6)
C6	0.0260 (7)	0.0261 (7)	0.0265 (7)	-0.0038 (6)	-0.0065 (6)	-0.0059 (6)
C7	0.0236 (7)	0.0189 (6)	0.0220 (6)	-0.0085 (5)	-0.0007 (5)	-0.0056 (5)
C8	0.0256 (7)	0.0230 (7)	0.0251 (7)	-0.0087 (5)	-0.0058 (5)	-0.0012 (5)
C9	0.0336 (8)	0.0394 (8)	0.0220 (7)	-0.0149 (6)	-0.0033 (6)	-0.0039 (6)
C10	0.0283 (8)	0.0575 (10)	0.0280 (8)	-0.0113 (7)	0.0033 (6)	-0.0130 (7)
C11	0.0228 (7)	0.0564 (10)	0.0349 (8)	-0.0029 (7)	-0.0048 (6)	-0.0100 (7)
C12	0.0274 (7)	0.0349 (8)	0.0237 (7)	-0.0071 (6)	-0.0068 (6)	-0.0045 (6)
C13	0.0262 (7)	0.0250 (7)	0.0248 (7)	-0.0112 (5)	-0.0067 (5)	-0.0035 (5)
C14	0.0272 (7)	0.0221 (6)	0.0236 (7)	-0.0088 (5)	-0.0105 (5)	-0.0043 (5)
C15	0.0297 (7)	0.0246 (7)	0.0247 (7)	-0.0080 (6)	-0.0082 (6)	-0.0042 (5)
C16	0.0297 (8)	0.0454 (9)	0.0289 (8)	-0.0093 (7)	-0.0061 (6)	-0.0139 (7)
C17	0.0337 (8)	0.0429 (9)	0.0492 (10)	0.0049 (7)	-0.0182 (7)	-0.0290 (8)
C18	0.0472 (9)	0.0217 (7)	0.0557 (10)	-0.0003 (7)	-0.0299 (8)	-0.0121 (7)
C19	0.0406 (8)	0.0224 (7)	0.0341 (8)	-0.0122 (6)	-0.0180 (7)	-0.0009 (6)
C20	0.0202 (6)	0.0219 (6)	0.0225 (6)	-0.0043 (5)	-0.0064 (5)	-0.0034 (5)
C21	0.0224 (6)	0.0222 (6)	0.0207 (6)	-0.0065 (5)	-0.0073 (5)	-0.0042 (5)
C22	0.0256 (7)	0.0264 (7)	0.0276 (7)	-0.0031 (6)	-0.0061 (6)	-0.0036 (6)
C23	0.0378 (8)	0.0240 (7)	0.0338 (8)	-0.0063 (6)	-0.0127 (7)	0.0031 (6)
C24	0.0366 (8)	0.0352 (8)	0.0230 (7)	-0.0183 (6)	-0.0067 (6)	0.0003 (6)
C25	0.0266 (7)	0.0367 (8)	0.0237 (7)	-0.0104 (6)	-0.0033 (6)	-0.0090 (6)
C26	0.0252 (7)	0.0236 (7)	0.0242 (7)	-0.0047 (5)	-0.0063 (5)	-0.0054 (5)

Geometric parameters ( $\text{\AA}$ ,  $^\circ$ )

P1—O1	1.4578 (10)	C12—H12A	0.9500
P1—O2	1.5916 (9)	C13—C14	1.5127 (18)
P1—O3	1.5948 (10)	C13—H13A	0.9900
P1—N1	1.6232 (11)	C13—H13B	0.9900
O2—C1	1.4092 (15)	C14—C19	1.3893 (19)
O3—C7	1.4096 (15)	C14—C15	1.3907 (19)
N1—C13	1.4693 (17)	C15—C16	1.383 (2)
N1—C20	1.4707 (17)	C15—H15A	0.9500
C1—C2	1.378 (2)	C16—C17	1.388 (2)
C1—C6	1.3826 (19)	C16—H16A	0.9500
C2—C3	1.386 (2)	C17—C18	1.378 (3)

C2—H2A	0.9500	C17—H17A	0.9500
C3—C4	1.382 (2)	C18—C19	1.387 (2)
C3—H3A	0.9500	C18—H18A	0.9500
C4—C5	1.382 (2)	C19—H19A	0.9500
C4—H4A	0.9500	C20—C21	1.5151 (18)
C5—C6	1.3913 (19)	C20—H20A	0.9900
C5—H5A	0.9500	C20—H20B	0.9900
C6—H6A	0.9500	C21—C22	1.3881 (19)
C7—C8	1.3760 (19)	C21—C26	1.3919 (18)
C7—C12	1.3791 (19)	C22—C23	1.393 (2)
C8—C9	1.3880 (19)	C22—H22A	0.9500
C8—H8A	0.9500	C23—C24	1.381 (2)
C9—C10	1.382 (2)	C23—H23A	0.9500
C9—H9A	0.9500	C24—C25	1.384 (2)
C10—C11	1.384 (2)	C24—H24A	0.9500
C10—H10A	0.9500	C25—C26	1.384 (2)
C11—C12	1.384 (2)	C25—H25A	0.9500
C11—H11A	0.9500	C26—H26A	0.9500
O1—P1—O2	115.77 (5)	N1—C13—H13A	108.8
O1—P1—O3	116.27 (5)	C14—C13—H13A	108.8
O2—P1—O3	97.78 (5)	N1—C13—H13B	108.8
O1—P1—N1	113.54 (6)	C14—C13—H13B	108.8
O2—P1—N1	104.31 (5)	H13A—C13—H13B	107.7
O3—P1—N1	107.44 (5)	C19—C14—C15	118.94 (13)
C1—O2—P1	122.79 (8)	C19—C14—C13	120.19 (12)
C7—O3—P1	119.73 (8)	C15—C14—C13	120.80 (12)
C13—N1—C20	115.99 (10)	C16—C15—C14	120.52 (13)
C13—N1—P1	121.10 (9)	C16—C15—H15A	119.7
C20—N1—P1	122.88 (9)	C14—C15—H15A	119.7
C2—C1—C6	121.90 (12)	C15—C16—C17	120.07 (15)
C2—C1—O2	116.55 (12)	C15—C16—H16A	120.0
C6—C1—O2	121.40 (12)	C17—C16—H16A	120.0
C1—C2—C3	118.83 (13)	C18—C17—C16	119.78 (14)
C1—C2—H2A	120.6	C18—C17—H17A	120.1
C3—C2—H2A	120.6	C16—C17—H17A	120.1
C4—C3—C2	120.38 (14)	C17—C18—C19	120.22 (14)
C4—C3—H3A	119.8	C17—C18—H18A	119.9
C2—C3—H3A	119.8	C19—C18—H18A	119.9
C5—C4—C3	120.03 (13)	C18—C19—C14	120.47 (14)
C5—C4—H4A	120.0	C18—C19—H19A	119.8
C3—C4—H4A	120.0	C14—C19—H19A	119.8
C4—C5—C6	120.37 (13)	N1—C20—C21	112.18 (10)
C4—C5—H5A	119.8	N1—C20—H20A	109.2
C6—C5—H5A	119.8	C21—C20—H20A	109.2
C1—C6—C5	118.49 (13)	N1—C20—H20B	109.2
C1—C6—H6A	120.8	C21—C20—H20B	109.2
C5—C6—H6A	120.8	H20A—C20—H20B	107.9

C8—C7—C12	122.33 (12)	C22—C21—C26	118.74 (12)
C8—C7—O3	120.00 (12)	C22—C21—C20	120.71 (12)
C12—C7—O3	117.59 (12)	C26—C21—C20	120.54 (11)
C7—C8—C9	118.41 (13)	C21—C22—C23	120.54 (13)
C7—C8—H8A	120.8	C21—C22—H22A	119.7
C9—C8—H8A	120.8	C23—C22—H22A	119.7
C10—C9—C8	120.28 (14)	C24—C23—C22	120.13 (13)
C10—C9—H9A	119.9	C24—C23—H23A	119.9
C8—C9—H9A	119.9	C22—C23—H23A	119.9
C9—C10—C11	120.20 (14)	C23—C24—C25	119.63 (13)
C9—C10—H10A	119.9	C23—C24—H24A	120.2
C11—C10—H10A	119.9	C25—C24—H24A	120.2
C12—C11—C10	120.16 (14)	C24—C25—C26	120.35 (13)
C12—C11—H11A	119.9	C24—C25—H25A	119.8
C10—C11—H11A	119.9	C26—C25—H25A	119.8
C7—C12—C11	118.61 (13)	C25—C26—C21	120.60 (13)
C7—C12—H12A	120.7	C25—C26—H26A	119.7
C11—C12—H12A	120.7	C21—C26—H26A	119.7
N1—C13—C14	113.73 (11)		

*Hydrogen-bond geometry (Å, °)*

*Cg1*, *Cg2* and *Cg3* are the centroids of the C1–C6, C14–C19 and C7–C12 rings, respectively.

<i>D</i> —H... <i>A</i>	<i>D</i> —H	H... <i>A</i>	<i>D</i> ... <i>A</i>	<i>D</i> —H... <i>A</i>
C2—H2 <i>A</i> ... <i>CG1</i> <sup>i</sup>	0.95	3.50	3.9798 (13)	114
C13—H13 <i>B</i> ... <i>CG1</i> <sup>ii</sup>	0.99	3.49	4.2048 (13)	131
C18—H18 <i>A</i> ... <i>CG3</i> <sup>ii</sup>	0.95	3.22	3.8839 (15)	128
C8—H8 <i>A</i> ... <i>CG2</i> <sup>iii</sup>	0.95	3.41	3.7716 (14)	106
C6—H6 <i>A</i> ...O1	0.95	2.51	3.1488 (17)	125

Symmetry codes: (i)  $-x, -y+1, -z+1$ ; (ii)  $x, y-1, z$ ; (iii)  $-x+1, -y, -z$ .